Adama Science and Technology University

A Research Project **Final Report**

Investigation of High Performance Solar Driers

By: - Dr. Addisu Bekele

Asst. Professor of Thermal Engineering
School of Mechanical Chemical and Materials Engineering
Tel: 0911 872362
Email: addisu2009@gmail.com; addisu2005@yahoo.com

March 01, 2019

Abstract

It is well known that the thermal performances of solar air collectors are very poor due to low thermal conductivity of air. Therefore, the intention of this research work is to investigate high performance solar air collector that can be used in drying agricultural products like tomato, onion, coffee, banana, etc. so that the drying efficiency will be improved, good quality of product can be obtained and the economy of the farmer as well as the country can be improved.

Optimum obstacle shape and geometry and arrangement has been obtained via numerical simulation using ANSYS FLUENT software and further experimental test is conducted in drying tomato and onion in ASTU and coffee drying at Jimma.

The solar driers have been manufactured from wood and metal and the both of them have been tested and a better performance have been obtained for the one made from metal because additional solar radiation ise absorbed by the drying chamber surface.

Detail experimental work has been done on onion and tomato and thus various test results have been recorded and reported here.

After an intensive experimental study out of the total 15 solar driers manufactured (11 by the fund from Finland Embassy and 4 by the fund from ASTU), 13 solar driers of higher efficiency with the obtained optimum obstacles arrangement and configuration have been disseminated to 4 different areas in the country in collaboration with Finland Embassy in Addis Ababa.

Acknowledgement

I would like convey my deep gratitude to ASTU for the financial support of this research work and staff of the Mechanical and Vehicle Engineering Department for their support in manufacturing and testing the solar driers. Here I would like to give my especial thank to Mr. Dereje W/georgis and Nasir Detamo and Sintayehu Shiferaw.

At last but not least I would like to acknowledge the staff of the then Wood Engineering Department of ASTU and a graduated student Mr. Negash for their support in manufacturing the solar driers from wood.

Table of Contents

List of Figures

List of Tables

1. Introduction

1.1 Background and Justification of the project

Food preservation is a process of treating and handling food to stop or slow down spoilages like loss of quality, edibility or nutritional value. Thus, food preservation allows for longer storage. Some of the commonly used preservation methods include: irradiation, food processing, drying, canning, cooling, modified atmosphere packaging and so on.

Drying is a method of food preservation that works by removing water from the food. The removal of moisture prevents the growth and reproduction of microorganisms responsible for decay and reduces the moisture mediated deterioration reactions. Drying brings about substantial reduction in weight and volume of products minimizing packaging, storage and transportation costs. It enables storability of products under ambient temperatures. Drying is excellent for most fruits and vegetables.

Dryers with solar air heater are the indirect or convection dryers in which the product is exposed to warm air which is heated by means of a solar absorber, or heat exchanger. Trays are arranged so as to induce air circulation. Measuring devices and control may also be incorporated to facilitate air renewal in the system. Fans and internal recycling are usually placed inside the chamber to allow the air flux to be uniform. The drying system is equipped with solar collectors made of blackened copper / galvanized iron plate, protected by a glass cover, which also helps to decrease heat losses. Solar drying does generate higher air temperature and thus lower relative humidity which are both conducive to improve drying rates, and better lower final moisture content of the dried crops. Hence, the risk of spoilage is reduced both during the actual process and in subsequent storage. The higher temperatures are also a deterrent to insect and microbial infestation. Additionally, protection against dust, insects and other animals is enhanced by drying in an enclosed structure. All these factors contribute to an improved and more consistent product quality.

Solar drying is faster because inside the dryer it is warmer than outside. It is labour saving as the product can be left in the dryer overnight or during rain. The quality of the product is better in terms of nutrients, hygiene and colour. However, solar drying is limited in the developing countries because of cost, which may be expensive.

1.2 Statement of the Problem

Flat plate collectors have been used to deliver heated air for crop drying and similar applications requiring air at low-to-medium temperature. The thermal efficiency of a smooth duct flat plate solar air hater is lower than that of a solar water heater because of a low value of heat transfer coefficient between the absorber plate and the air flowing through the collector duct. This leads to a high operating temperature of the collector, especially the absorber plate, resulting in greater heat loss from the collector. Hence, the researchers have directed their efforts towards enhancement of heat transfer coefficient by creating turbulence near the heat transferring surface.

Due to this poor efficiency of collector, unavailability of sun during night and difficulty of thermal storage; it is not yet common in Ethiopia to dry agricultural products using these solar driers. Therefore, the intention of this research work is to investigate high performance solar air collector using inclined, curved/twisted delta shaped obstacles mounted on the absorber plate with different configuration so that the drying efficiency will be improved and it can be used in drying agricultural products like coffee, onion, banana, etc.

1.3. Objectives

The general objective of this research work is to investigate high performance solar air collector for drying of agricultural products

1.3.1 Specific Objectives

The specific objectives of this research project are:

- To numerically study the effect of various shaped tabulators/ obstacles on heat transfer enhancement in solar air heaters.
- Obtain an optimum obstacle geometry and arrangements that can maximize the drying efficiency.
- To design, manufacture and test a solar drier system.
- To design and manufacture a solar collector with obstacles mounted.
- To design and manufacture drying chamber with fan installed.
- To study the drying effect of the solar drier for tomato, onion and etc.

1.4. Significance & Beneficiaries

The beneficiaries of this research work are the farmers, the university (teachers, students, and technicians) and the country as a whole.

The benefits of this research work are:-

- ✓ The multipurpose solar drier produced will be used in drying d/t agricultural produce like coffee, onion, mango, banana, etc.
- ✓ The quality of the product dried by this device will be higher than the traditional sun drying
- ✓ The quantity loss during traditional sun drying will be totally absent
- ✓ The economic income of the farmer will improved.
- ✓ The labor intensive work in case of traditional sun drying will be much reduced by using this device.

1.5 The research outcome are basically

- → Obtaining a high efficient solar dryer by increasing the heat transfer from the absorber to the air stream passing under it. This used different tarbulators / obstacles of different geometries and arrangements. Thus after an intensive experimental work optimum obstacle geometry and arrangements have been obtained that has maximized the efficiency of the driers.
- → These high solar driers have been used to dry tomato, onion, coffee and other fruits and vegetables in order to store it for a long time. It has also a great benefit in minimizing post-harvest loss of these agricultural produces and play a significant role in food security and product quality. In collaboration with Finland Embassy in Addis Ababa 15 Solar driers have been manufactured and 13 of them have been disseminated to farmers while 2 of them left in university for further research study and also for educational purpose. The cost of 11 dryers are covered by Finland Embassy fund whereas 4 collectors cost are covered by ASTU fund.

The dissemination of these solar driers have been done to the community in collaboration with Finland Embassy in Addis Ababa. The target group of these beneficiaries are: woman farmers, disabilities and HIV patients on date Nov. 23, 2015 in the following sites:

1. East Showa Zone
    - Bora Woreda, Doddo wadaraa Kebele – 6 driers
    - and Dugda Woreda, Bekele Girisaa Kebele – 3 driers
2. Jimma Zone
    - Manna Woreda, Haroo Kebele – 3 driers
3. AgroBig project (Fogera woreda Woreta city)
    - a project running under Finland Embassy – 1 drier

These solar driers have been installed to these site and training had been given to the users.

2. Literature Review

Till now so many researchers have tried so many mechanisms to improve the efficiency of solar collectors. Among these some of the mechanisms are by:

- Using fins – to increase the convective heat transfer coefficient
- Using Double glass cover – to minimize the heat loss
- Using multiple air flow path – to minimize the heat loss
- Using Packed bed – to increase the convective heat transfer coefficient
- Using Mesh wire – to increase the convective heat transfer coefficient
- Using artificial roughness – to increase the convective heat transfer coefficient
- Using obstacles – to increase the convective heat transfer coefficient

Solar Air Heaters with Obstacles

The purpose of introducing obstacles in the air channel is to create the turbulence, so as to increase the heat transfer coefficient and hence the collector's efficiency. In order to create the turbulence, obstacles must, for a given air flow rate; increase the speed of the air flowing in the collector. This can be achieved in part by blocking the path for the flowing air through the use of transversal and longitudinal obstacles.

Besides the action on the choice of insulator, the absorber, and slope angle of collector, the choice of the type of obstacles allowing a better heat transfer from the absorber to the moving air can be assured by:

- Avoiding the creation of dead zones (the air should pass in the totality of the collector).
- Sending the moving air towards the absorber and not towards the insulator.
- Fixing the obstacles on the absorber to benefit from the wings effect.
- Placing the obstacles following a close spacing to create the turbulence even at low air flow rates.

Gbaha (1989) studied the effect of delta wing-shaped baffles (Fig. 1), placed as a replacement for small transversal baffles fixed on the absorber plate. The caloporting air attacks the baffles at their base. He also placed delta wing-shaped baffles with 26 transversal rows each including nine delta wings with wing angle of 60°, incidence 140° with regard to air flow. Finally, he verified the advantage of a selective absorber over the absorber painted black.

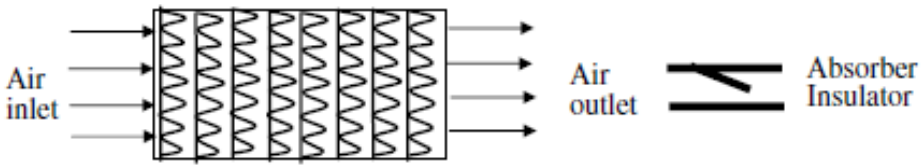

Fig. 1 Collector with delta wing-shaped baffles (Gbaha 1989)

Hachemi (1992) studied especially the placing of delta wing-shaped and rectangular baffles in close order fixed to the absorber, thus playing the role of wings besides the aeraulic effect. The importance of placing an aluminum plate, painted in black, in the air channel on the side of the insulator thus warming the internal face of the insulator to avoid the cooling of the moving air in its contact was also investigated.

Moummi (1994) studied in particular, rectangular baffles fixed on the insulator but the upper half of which are inclined, thus directing caloporting air towards the absorber and creating a strong local turbulence. The objective is thus reached: link of the caloporting air to the absorber for a better heat transfer.

Moummi (1995) further studied the spacing of the small transversal baffles placed on the insulator and assembled in quincunx. The increase in frequency leads to an increase in efficiency and also an increase in the pressure loads. It is necessary to optimize their number according to the air flow rate and the desired efficiency.

Alvarez et al. (2004) has designed and tested a new type of double flow SAH with an absorber plate made of recyclable aluminum cans as shown in Fig. 2. The experimental result show an increase in efficiency up to 74% of the solar air collector using recyclable aluminum cans and is technically and economically feasible. The advantages of using recyclable materials to build absorber plates of air solar collector imply to have cheaper absorbers and cleaner environment.

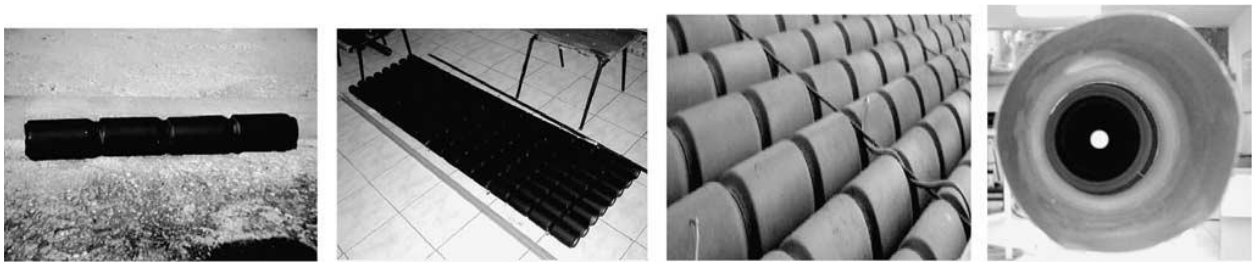

Fig. 2 Recyclable aluminium cans absorber plate (Alvarez et al. 2004)

Moummi et al. (2004) further used obstacles made from rectangular plate fins mounted on the back wooden plate and inserted perpendicular to the flow as shown in Fig. 3. The fluid flows out through the interstices between fins in the same row allows a good distribution of the fluid, reduces the dead zone and increases turbulence as a result the efficiency factor of the solar collector is improved.

Abene et al. (2004) have studied the improvement of the efficiency–temperature rise couple of the flat plate solar collector for drying of agricultural product yellow onion by considering several types of obstacles disposed in rows in the dynamic air vein of the flat plate collector. The different shapes studied are ogival transverse (OT), ogival inclined folded (OIF), waisted tube (WT), waisted delta lengthways (WDL), waisted ogival lengthways (WOL) and transverse-longitudinal obstacles (TL). By comparing with the collector without obstacles (WO), the thermal transfers and, consequently, the output temperature (TOC) and the collector efficiency (η) are clearly improved. The best two systems, waisted delta lengthways (WDL) and transverse longitudinal (TL) are used for drying the agricultural product.

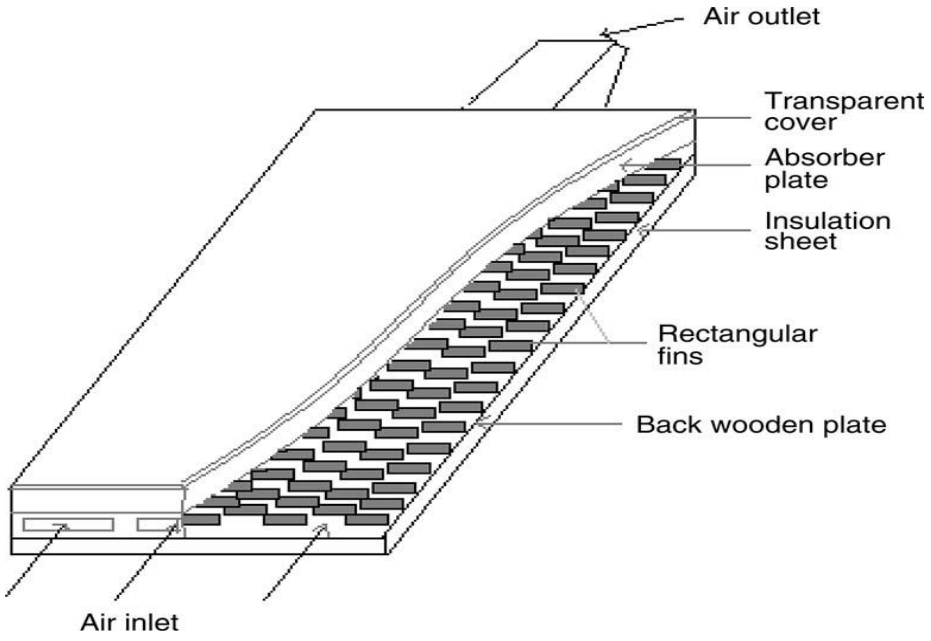

Fig. 3 Collector with finned system on the back wooden plate (Moummi et al. 2004)

From the results obtained for different solar collectors types examined, the introduction of obstacles in the air channel is a very important factor for the improvement of collector

performance. However, the form, dimensions, orientation and disposition of the obstacles considerably influences the collector efficiency. The losses of load (pressure drop) are acceptable in all cases due to the transversal and longitudinal spaces between the obstacles of the same row and that of successive rows, respectively.

Ben Slama (2007), were interested in the creation of turbulence in the air channels by using baffles. The studies on various types of baffles placed in the air passage are made in three stages: visualization of air flow, measurement of the pressure drop, and determination of the energetic efficiency by measuring the increase in temperature of the caloporting air at a given flow rate and under a given solar irradiance.

The types of baffles studied are:

- Placed transversally or longitudinally with regard to the collector.
- Occupying totally or partially the width of the collector.
- Placed on the insulator or fixed at the absorber (in the latter case, baffles act as wings).
- Occupying totally or partially the thickness of the air vein (in the first case they block the air flow rate in their place).
- Rectangular or in the shape of delta wings.

The efficiency reached 80% for an air flow rate of 50 $m^3/h/m^2$, allowing a temperature increase of 70°C to be achieved.

Esen (2008) experimentally studied the influences of various parameters, such as the obstacle types, the mass flow rate of air and the level of absorber plates in duct, on the energetic and exergetic efficiencies of double-flow SAH as shown in Fig. 4 and the results show that the largest irreversibility is occurring at the flat plate (without obstacles) collector in which collector efficiency is the smallest.

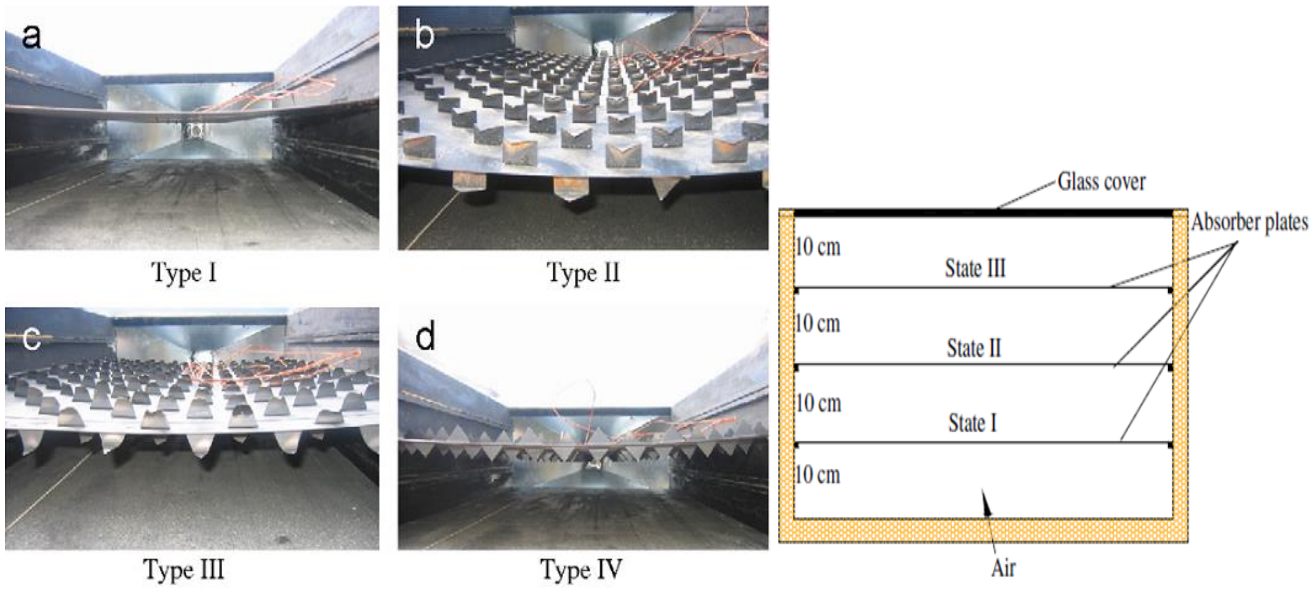

Fig. 4 Schematic assembly of the front view of collector (Esen 2008)

The optimal value of efficiency gained when the collector is at the middle level (State-II) and for all operating conditions results yield higher efficiency values for Type III collector than the other types of collectors.

Ozgen et al. (2009) studied the thermal performance of SAHs in which aluminum cans of different arrangements are used as an obstacle and the result is compared with that of smooth type (without obstacles) as shown in Fig. 5. According to the results of the experiments, the double-flow type of the SAHs with aluminum cans has been introduced for increasing the heat-transfer area, leading to improved thermal efficiency. Testing results always yield higher efficiency values of the type I (non-arranged cans) than that of the type III (without cans) flat-plate collector. The obstacles or cans ensure a good air flow over and under the absorber plates, create the turbulence and reduce the dead zones in the collector.

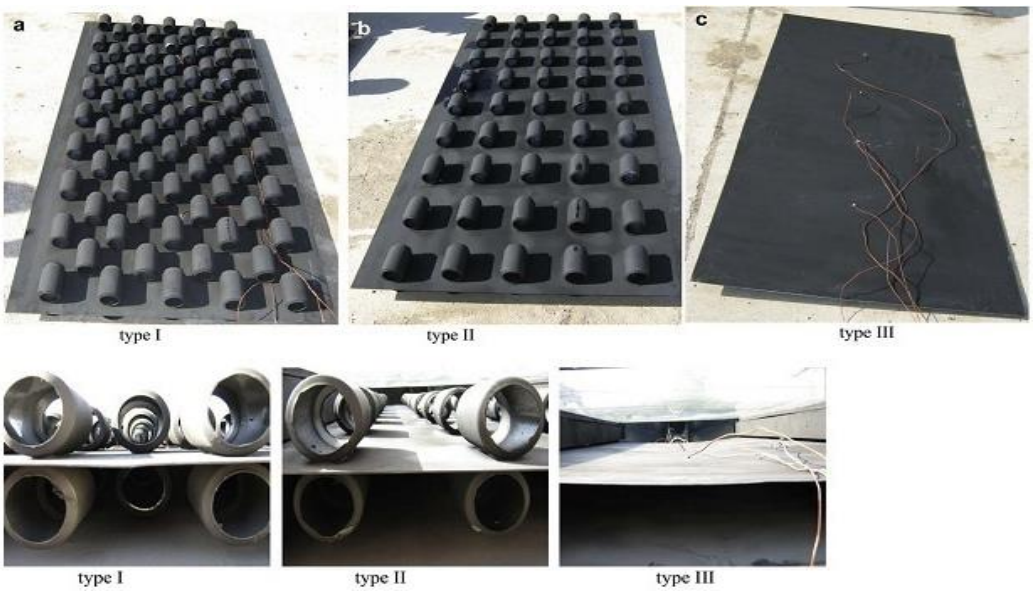

Fig. 5 Types of absorber plates and the view of absorber plates in the collector box, (a) type I, (b) type II, (c) type III (Ozgen et al. 2009).

3. Methodology

The general methodology used in conducting this research work is

3.1 Data Collection

Various thermos physical properties of fruits and vegetables has been collected and analyzed with the weather condition of Adama and nearby. Also various collector data has been collected from local market.

3.2 System Design

The complete solar drier system, both the collector part and the drying chamber has been designed as shown in Fig. 6.

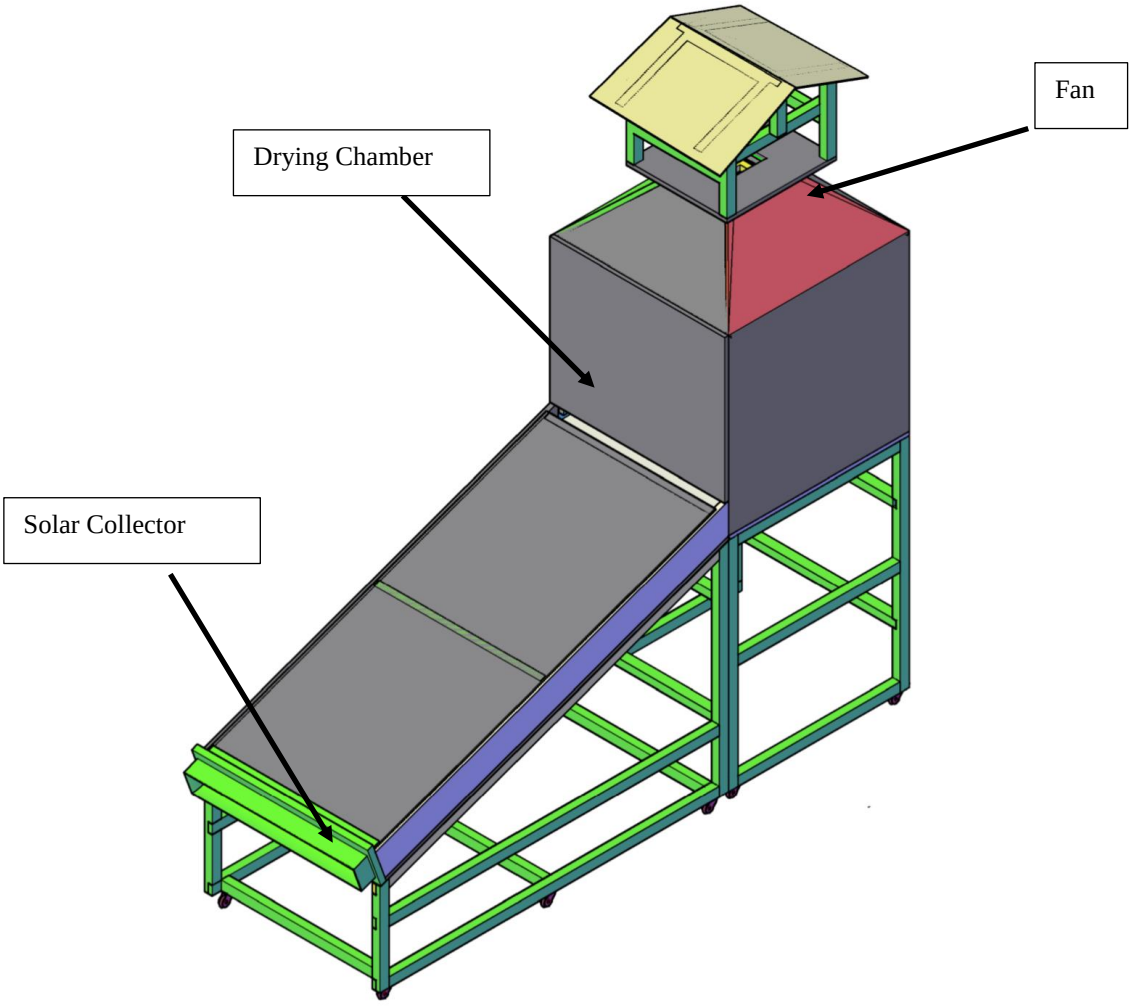

Fig. 6 Schematic diagram of the designed solar drier

- ✓ The manufacturing of the solar drier is held in Mechanical & Vehicle Engineering and Wood Engineering department workshops of ASTU.

3.3 Parametric study using numerical simulation (using CFD Software)

A three dimensional CFD analysis of fluid flow and heat transfer characteristics in a rectangular duct having delta shaped obstacles mounted on one surface, is done. One of the four walls of the duct is provided with obstacles and subjected to a constant heat flux while other walls are smooth and insulated. The selection of suitable turbulence model used for analysis has been carried out in three steps:

1. The preliminary selection of suitable turbulence models from literature.
2. Selection of suitable models from amongst the first proposed models after being applied to smooth duct and comparing the result with standard correlations available.
3. The final selection of the most suitable model from the models selected in step 2 after being used for the analysis of the obstacles mounted duct.

The parametric study using numerical simulation is done with the following procedures

i. Creating the Geometry

The geometry is created on GAMBIT preprocessor by "bottom up" approach. In bottom up approach, first the vertices are created in three-dimensional Cartesian coordinate system. Then connecting these vertices, edges are formed. From these edges, faces are created and finally the volume of the flow model is created from these faces. It is quite impossible to construct and analyze the whole geometry of flow domain because of tremendous computational efforts required for this purpose. In this CFD analysis only a portion of the test section is modeled assuming the flow is fully developed at the point.

The computational model of the present physical domain (Fig. 7) is developed using GAMBIT 2.4 and the analysis is carried out using ANSYS FLUENT 12.1 commercial software package.

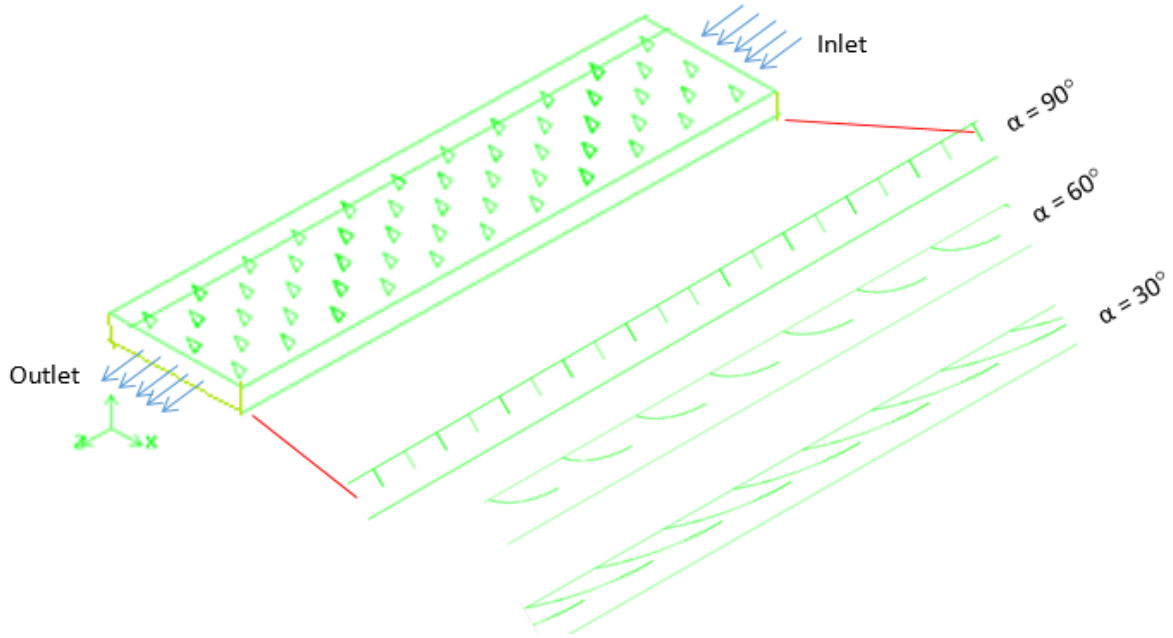

Fig. 7 computational model

ii. Meshing the Geometry

In order to accurately predict the result, the mesh near the obstacle should be very fine, thus a "fixed size function" is attached to all surfaces of the obstacles and to the absorber plate (Fig 8). Tetrahedral/Hybrid mesh element with T-Grid meshing scheme is used for meshing the model. The quality of the mesh is checked for equi-size skew and it is found to be below 0.75.

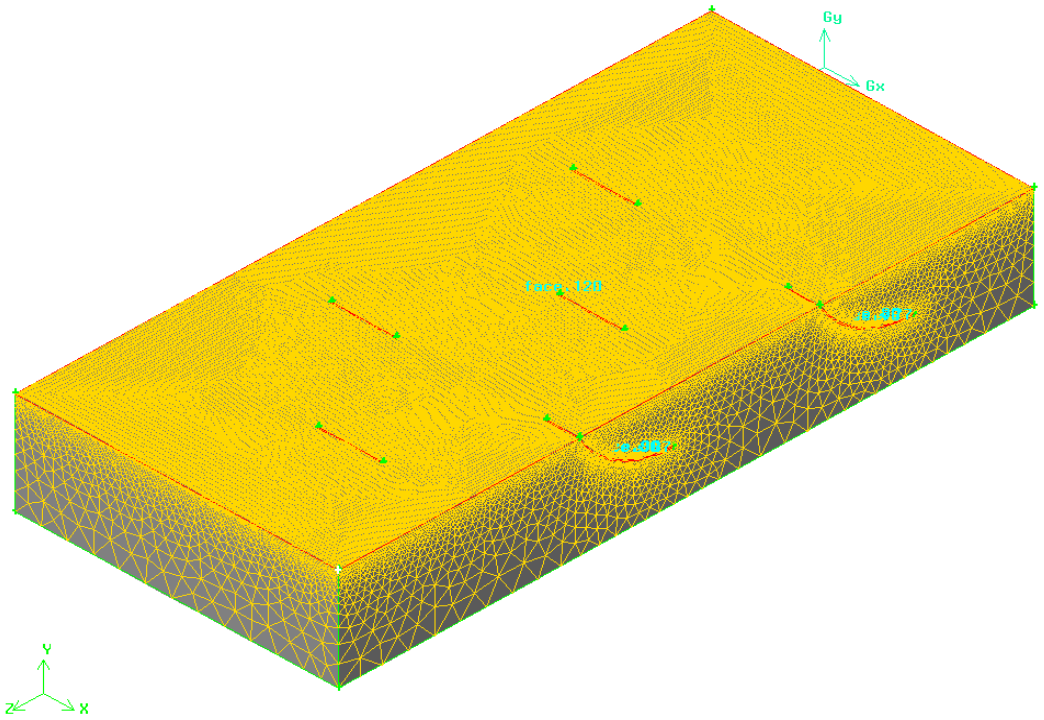

Fig. 8 Mesh of computational model (P_l/e = 3/2, P_t/b = 7/3, e/H = 0.50, α = 60°)

iii. Specifying the Boundary Types

The boundary types are specified at different faces as follows: "Velocity Inlet" for inlet face, "Pressure outlet" for outlet face, "Symmetry" for one side wall and "Wall" boundary conditions for the other faces. In specifying continuum types, panel fluid is selected for the model. Finally the mesh file is exported to the fluent solver.

iv. Solution Process

a) Problem Setting

Pressure-based (Segregated) solution method is used to discretize and solve the governing equations for steady state condition. This approach solves for a single variable field by considering all cells at the same time. It then solves for the next variable field by again considering all cells at the same time, and so on. Since this analysis includes the heat transfer effect, the energy option is set on to solve for energy equations.

Reviewing the various turbulence models to analyze turbulent flows, it is seen that the turbulence is basically modeled by a term μ_t (called eddy viscosity). Mostly modeling means to find ways and methods to evaluate μ_t.

Since the present analysis is concerned with heat transfer enhancement due to the obstacles mounted on broad heated wall of rectangular duct, the influencing parameters are both obstacle and flow field. Hence, to predict the heat transfer from the surface to the flowing fluid, the model should have capability to resolve the flow right down to the wall. Therefore, the following turbulent models are found to be suitable for the current type of studies. Standard k-ε model, Renormalization group (RNG) k-ε model, Realizable k-ε model, standard k-ω and Shear Stress Transport (SST) k-ω Model. These models are first used for smooth duct analysis as shown in the Fig. 9 and among these the best models approaching the standard correlations available in literature "Dittus Boelter correlation", are Standard k-ε model and Realizable k-ε model. These models are further used for obstacles mounted duct analysis and after the result is being compared with the experimental one, it is found that the Realizable k-ε model with enhanced wall treatment is best approaching the experimental result of the present study and used for the rest of analysis.

Dittus-Boelter Equation: $Nu_s = 0.024Re^{0.8}Pr^{0.4}$ for $10^4 \leq \text{Re} \leq 1.24 * 10^5$

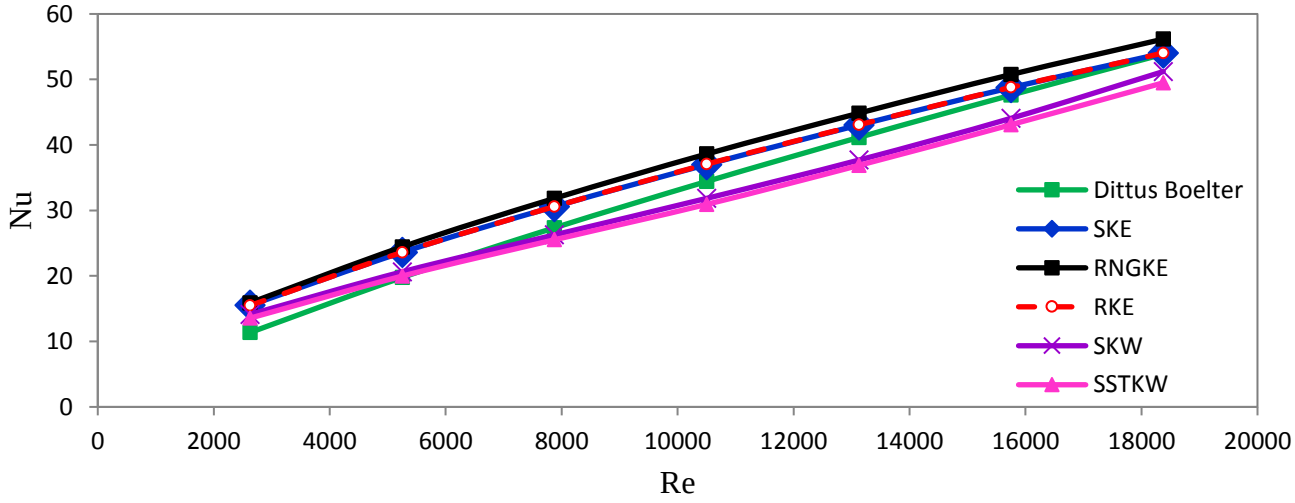

Fig. 9 **Smooth duct analysis for selection of suitable turbulent model**

Finally, the boundary condition is set for this model is as follows:

Uniform velocity at inlet, uniform temperature at inlet, outlet pressure (atmospheric pressure), constant heat flux ($q'' = 800\, W/m^2$) on broad top section of the test section and all other walls as adiabatic. In addition, turbulence intensity at inlet and hydraulic diameter of the model are also given.

b) Solution

SIMPLEC algorithm is used to compute the flow field by pressure velocity coupling method and second order upwind scheme is used for discretization of convective terms. During the solution process, the convergence is monitored dynamically by checking residuals and surface integrals. Surface heat transfer coefficient is used as a variable for monitoring surface integral. When this value stops changing, the iteration can be stopped. The convergence criteria used for monitoring the residuals is as given in Table 1. Finally the solution is initialized and the iteration will start.

The convergence plot of scaled residuals (Fig. 10) shows that after about 400 number of iteration the residuals are settled and continuously decrease and seems to become constant after 2000 number of iterations. The convergence history plot of surface heat transfer coefficient on the absorber plate (Fig. 11) shows that from 1200 - 2100 number of iteration the surface heat transfer coefficient remains constant showing that the solution is converged.

The Wall Y^+ on the absorber plate (Fig.12), which is less than 1.9 shows that the near wall mesh is fine enough and viscous sub layer is properly resolved. So the enhanced wall treatment method used for near-wall treatment is appropriate.

Table 1 Convergence criteria for monitoring residuals

S. No.	**Residual**	**Convergence Criteria**
1	Continuity	0.00001
2	X - Velocity	0.00001
3	Y - Velocity	0.00001
4	Z- Velocity	0.00001
5	Turbulent kinetic energy, k	0.00001
6	Specific dissipation rate, ε	0.00001
7	Energy balance	0.00001

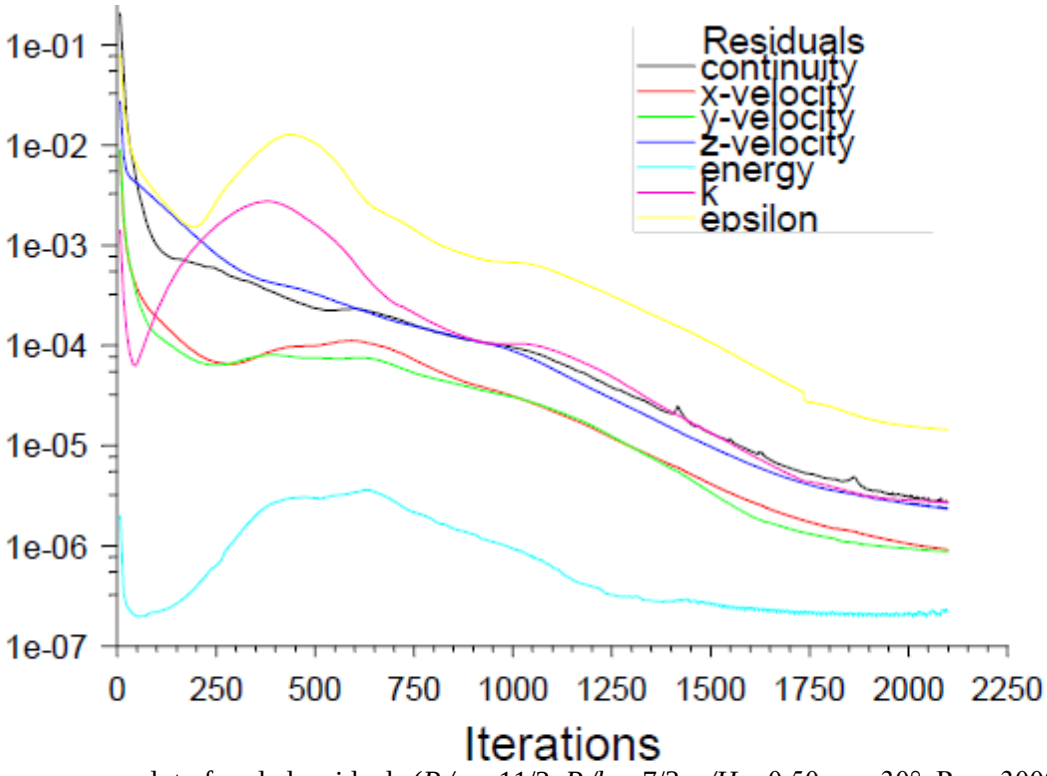

Fig. 10 Convergence plot of scaled residuals (P_l/e = 11/2, P_t/b = 7/3, e/H = 0.50, α = 30°, Re = 3000)

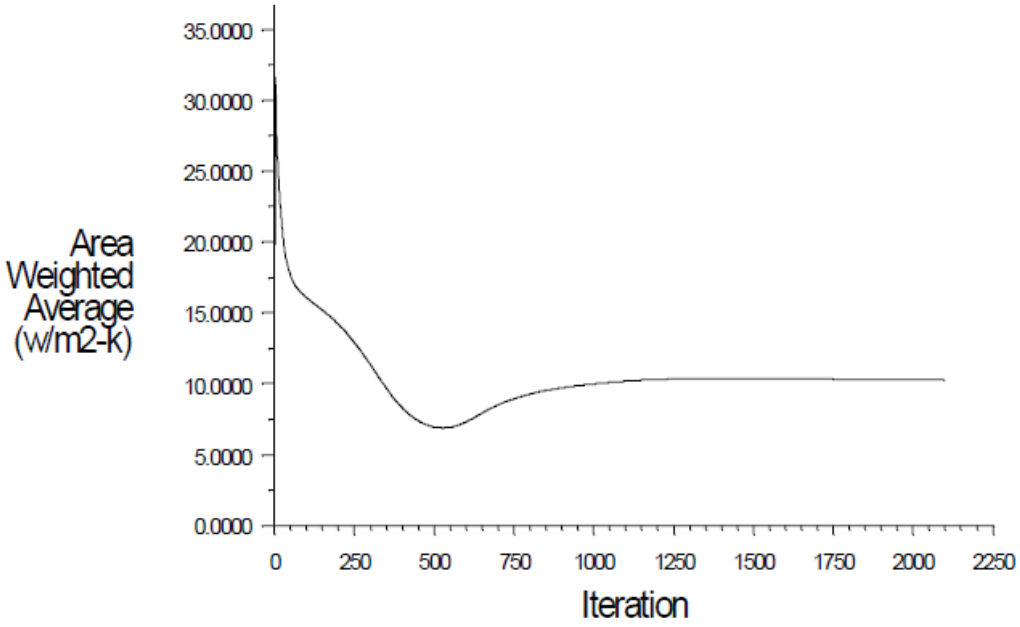

Fig. 11 Convergence history plot of Surface heat transfer coefficient on the absorber plate (P_l/e = 11/2, P_t/b = 7/3, e/H = 0.50, α = 30°, Re = 3000)

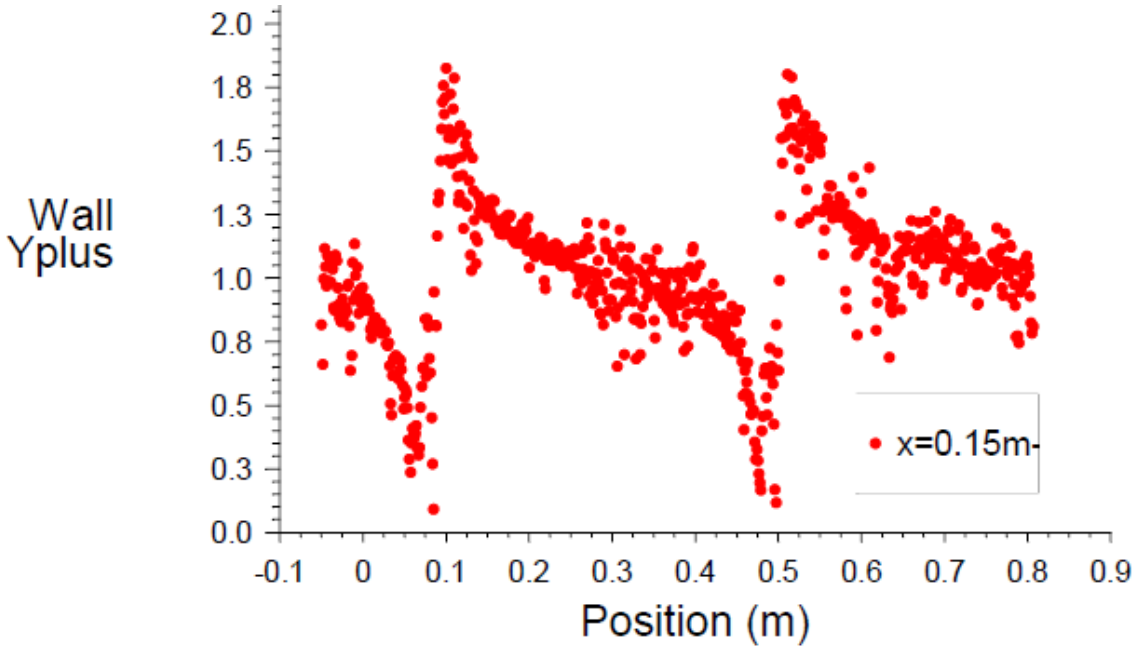

Fig. 12 Wall Y^+ plot on the center line of absorber plate (P_l/e = 11/2, P_t/b = 7/3, e/H = 0.50, α = 30°, Re = 3000)

c) Grid Independence

For grid independence test, a solution adaptive refinement method is used. By using solution-adaptive refinement, cells can be added where they are needed in the mesh, thus enabling the futures of the flow field to be better resolved. When adaption is used properly, the resulting mesh is optimal for the flow solution because the solution is used to determine where more cells need to be added. Thus, computational resources are not wasted by the inclusion of unnecessary cells, as it occurs in the structured grid approach. Also, the effect of mesh refinement on the solution can be studied without completely regenerating the mesh.

Sample grid independence test result for P_l/e = 11/2, P_t/b = 7/3, e/H = 0.50, α = 90 is given in Table 2. It shows that after about 2,488,032 numbers of cells, the variation in the value of convective heat transfer coefficient is negligible. Hence, the further analysis is carried out using mesh with 2,488,032 numbers of cells.

Table 2 Grid independence test result for P_l/e = 11/2, P_t/b = 7/3, e/H = 0.50, α = 90°

S/ No.	Number of Cells	Convective heat transfer coefficient, h [W/m^{2}K]
1	624967	4.46

2	1080577	5.013
3	1857752	5.847
4	**2488032 ***	**6.226**
5.	3117976	6.246

3.4 Manufacturing

The complete systems of the solar drier are manufactured from wood in wood engineering department (Fig. 13) and from metal in mechanical and vehicle engineering department workshops (Fig. 14).

a) Collector and drying chamber construction

b) Manufacturing of tray of the drier using galvanized wire mesh

c) Tabulators fixed and the absorber plate is black painted to maximize solar absorption

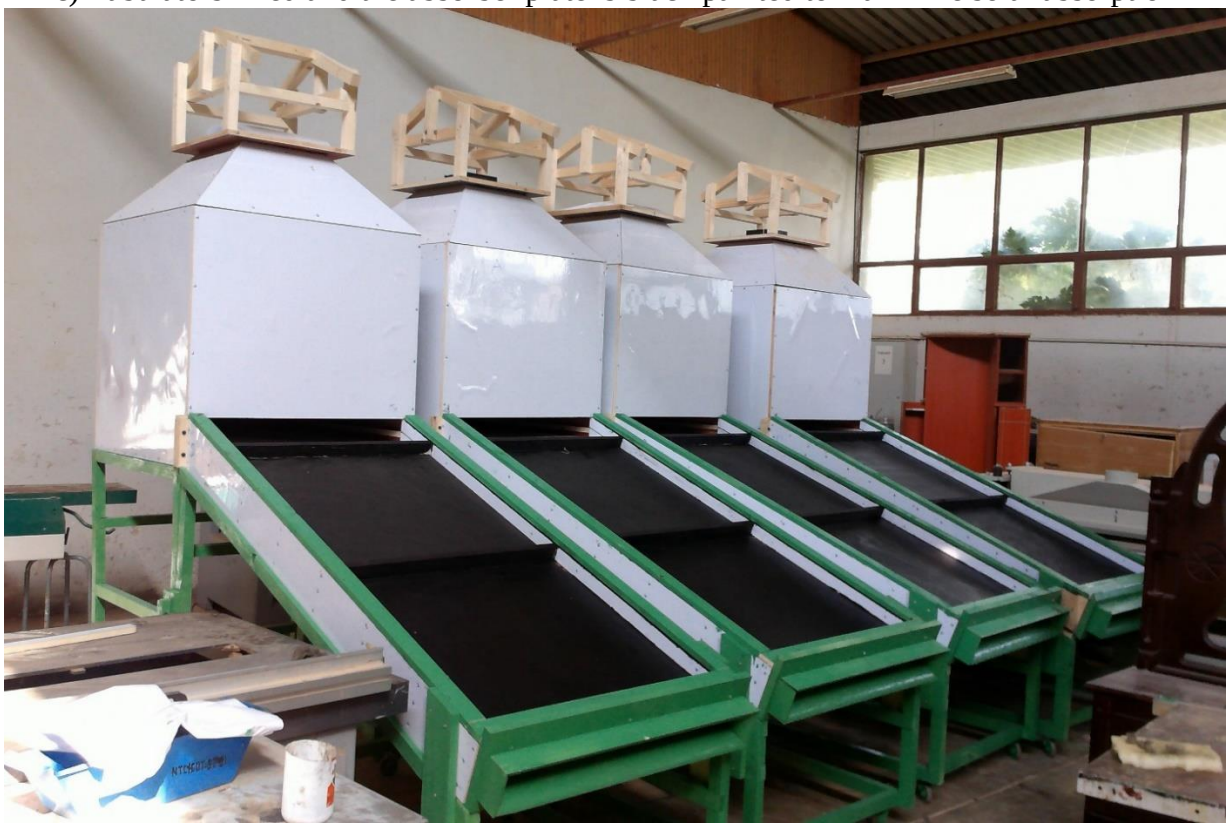

d) Assembled Solar Drier made of Wood

Fig. 13: Manufacturing of Solar Drier made of Wood

a) Manufacturing of the drying chamber

b) Manufacturing of the collector part

c) Manufacturing of the obstacles and planting it on the absorber plate

Fig. 14: Manufacturing of Solar Drier made of Metal

3.5 Testing

Obstacles geometry and range of parameters studied

Obstacles geometry

The shape and construction of the obstacles (Fig. 15) are simple and interesting. The choice of the geometrical shapes of the obstacles used ensures a good air flow over the absorber plate, create turbulence and reduce dead zones in the collector. The systematic and meticulous study considered concerns several different vein configurations of flow in the solar collectors. The detail geometries of obstacles used are given in Table 3.

Table 3 Detail geometry of obstacles

S. No.	h	e	α	r	β
1	146.6	37.5	30	279.9	11.68
2	97.7	25	30	186.6	17.46
3	48.9	12.5	30	93.3	34.11
4	78.5	37.5	60	75	21.64
5	52.4	25	60	50	31.95
6	26.2	12.5	60	25	59.58
7	37.5	37.5	90	-	43.60
8	25	25	90	-	61.93
9	12.5	12.5	90	-	100.39

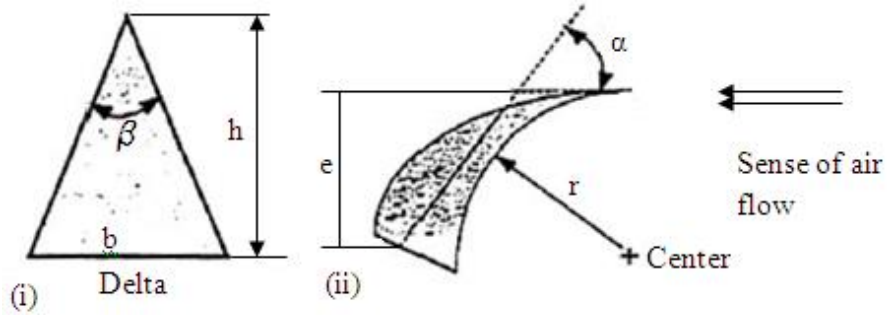

Fig. 15 Schematic diagram of: (i) obstacle before twisting, (ii) Obstacle after twisting

Ranges of parameters

Obstacle parameters are determined by obstacles height (e), obstacles base (b), obstacles longitudinal and transverse pitch (P_l & P_t) and obstacles twisting angle (angle of incidence) (α). The parameters have been expressed in the form of the following more general forms:

i. Relative obstacle height (e/H)
ii. Relative obstacles longitudinal pitch (P_l/e)
iii. Relative obstacles transverse pitch (P_t/b)
iv. Obstacles twisting angle (Angle of atack/Angle of incidence) (α)

The range of parameters for this study has been decided on the basis of practical considerations of the system and operating conditions of the solar air heater. The values of these obstacles parameters used for the numerical study are given in Table 4.

Table 4 Range of geometrical and operating parameters

S.No.	Obstacles and flow parameters	Range of parameters
1	Relative obstacle height (e/H)	0.25, 0.50, 0.75
2	Relative obstacle longitudinal pitch (P_l/e)	11/2, 7/2, 3/2
3	Relative obstacle transversal pitch (P_t/b)	7/3, 3/2, 1
4	Angle of attack (α)	90°, 60°, 30°

The range of relative obstacle height is selected on the basis of percentage of blockage in air flow in the channel with minimum 25% and maximum 75% blockage. The range of obstacle transversal and longitudinal pitch is selected on the basis of consideration of flow pattern observed through numerical analysis and also reported in literatures (Abene 2004, Esen 2008). Similarly the angle of twisting the obstacle or angle of attack is selected on the basis of diverting air flow to the absorber plate and creating turbulence.

Instrumentation

The following parameters are measured during the experiments.

- Temperature of air at inlet and outlet
- Temperature of absorber plate
- Solar radiation

K-type (Chromel (Ni-Cr alloy) / Alumel (Ni-Al alloy)) thermocouples of 0.315 mm wires diameter are used to measure the air and the heated plate temperatures at different locations.

The solar radiation is measured using the solar power meter borrowed form Bahir Dar University.

Fig. 16 Solar Power Meter used to measure radiation during testing of the solar drier

3.6 Dissemination

This research work output is targeted to be disseminated with beneficiaries identified from four different areas in the country.

4. Results and Discussion

4.1 Numerical Result

Since the main objective of this numerical analysis is to investigate the heat transfer and fluid flow phenomena over these delta-shaped obstacles some of the important results are plotted and discussed below. All figures are scaled up to show the flow structure clearly. The flow field is investigated in terms of voracity, velocity contour, and turbulent intensity. Heat transfer phenomenon is studied in terms of static temperature distribution and surface heat transfer coefficient for different obstacles configurations.

The flow filed can be visualized using the velocity contour plots as shown in Figs. 17, 18 and 19

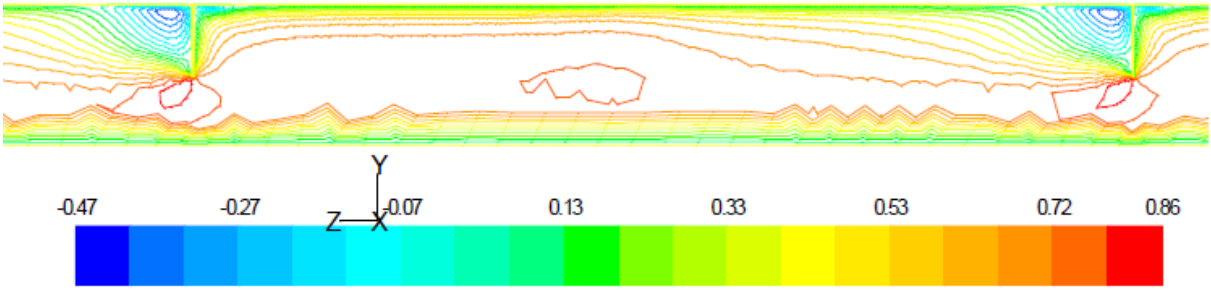

Fig. 17 Velocity contour for P_t/b = 7/3, e/H = 0.50, P_l/e = 11/2, Re = 3000, α = 90° obstacles

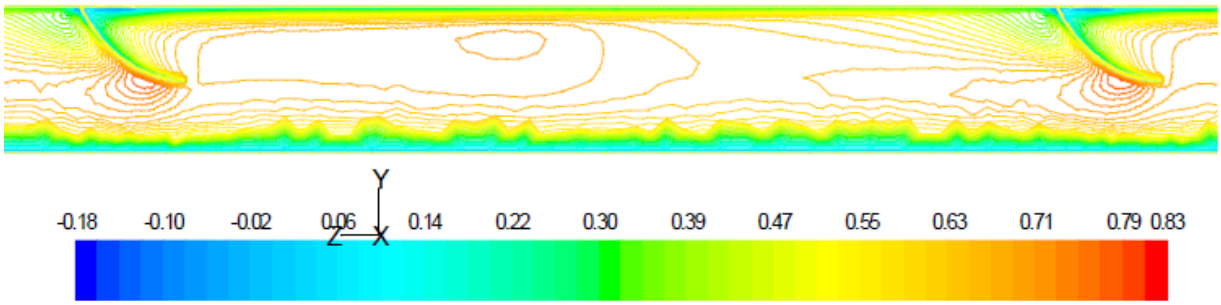

Fig. 18 Velocity contour for P_t/b = 7/3, e/H = 0.50, P_l/e = 11/2, Re = 3000, α = 60° obstacles

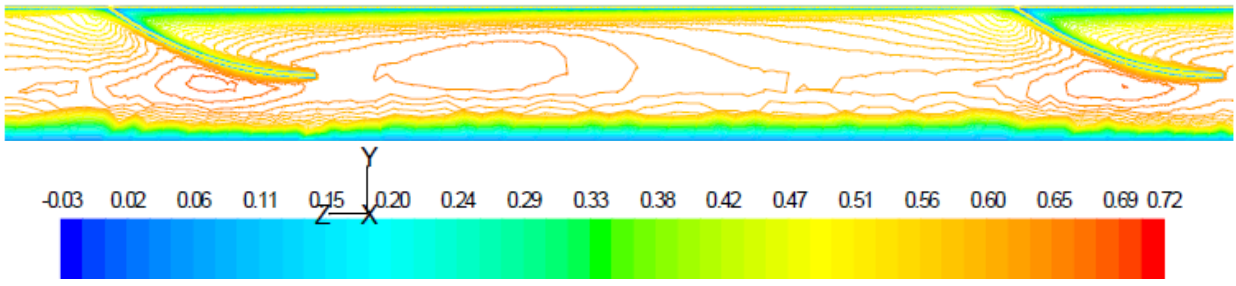

Fig. 19 Velocity contour for P_t/b = 7/3, e/H = 0.50, P_l/e = 11/2, Re = 3000, α = 30° obstacles

a) Effect of Vorticity, Turbulence Intensity and Obstacle Arrangement on Heat Transfer and fluid flow

Figs. 20, 21 and 22 show Vorticity Contour plot for angle of attack 90°, 60° and 30° respectively. The vortices generated were the result of the introduction or exploitation of secondary flows, rather than the manipulation or alteration of the main flow. The heat transfer enhancement consists of main-flow enhancement and secondary flow enhancement. Louvered fin, strip fin and wavy wall are examples of main-flow enhancement method. The intentional generation of vortices to enhance heat transfer is a secondary flow enhancement method.

In general there are two types of vortices: transverse vortex (TV) and longitudinal vortex (LV). The rotational direction of a transverse vortex is normal to the main flow direction and the flow is two-dimensional, whereas the longitudinal vortices have their rotating axes parallel to the main flow direction and the flow is three dimensional. In fact, it is impossible to generate pure longitudinal vortices, since transverse vortices are always generated at the same time. The predominance of one over the other depends on the attack angle α. For angle of attack of 90° (Fig. 20, mainly transverse vortices are generated and for angle of attack of 60° (Fig. 21) and 30° (Fig. 22), mainly longitudinal vortices are generated.

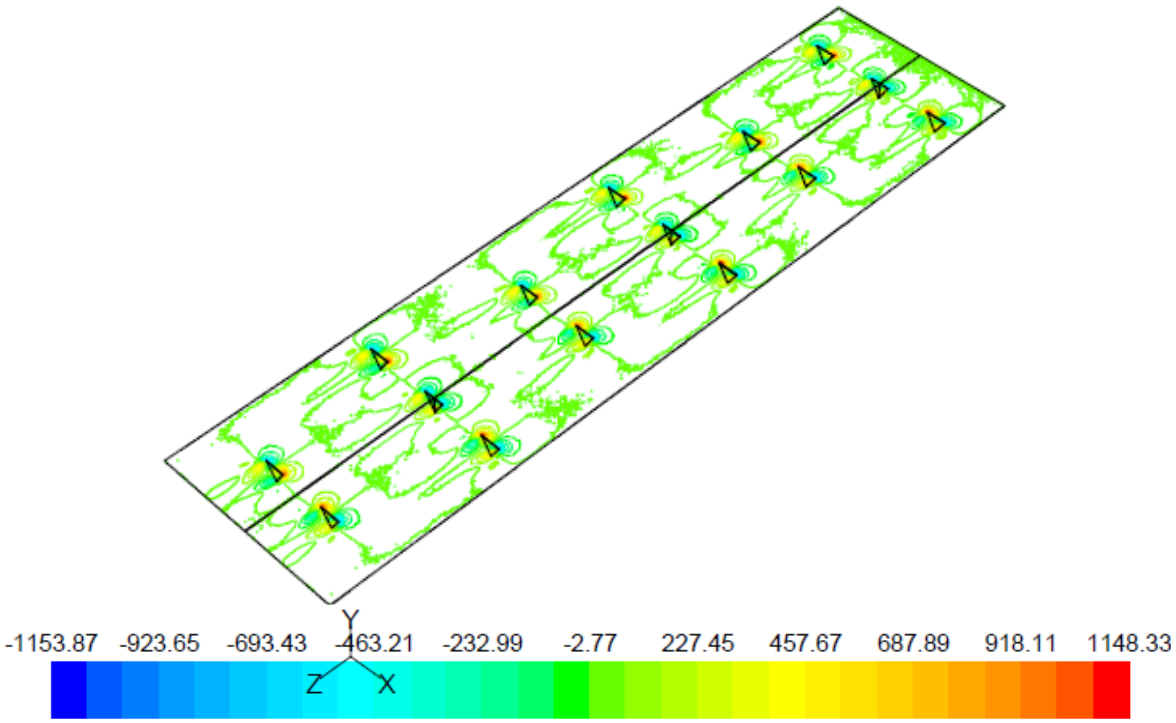

Fig. 20 Vorticity for P_t/b = 7/3, e/H = 0.50, P_l/e = 11/2, Re = 3000, α = 90° obstacles

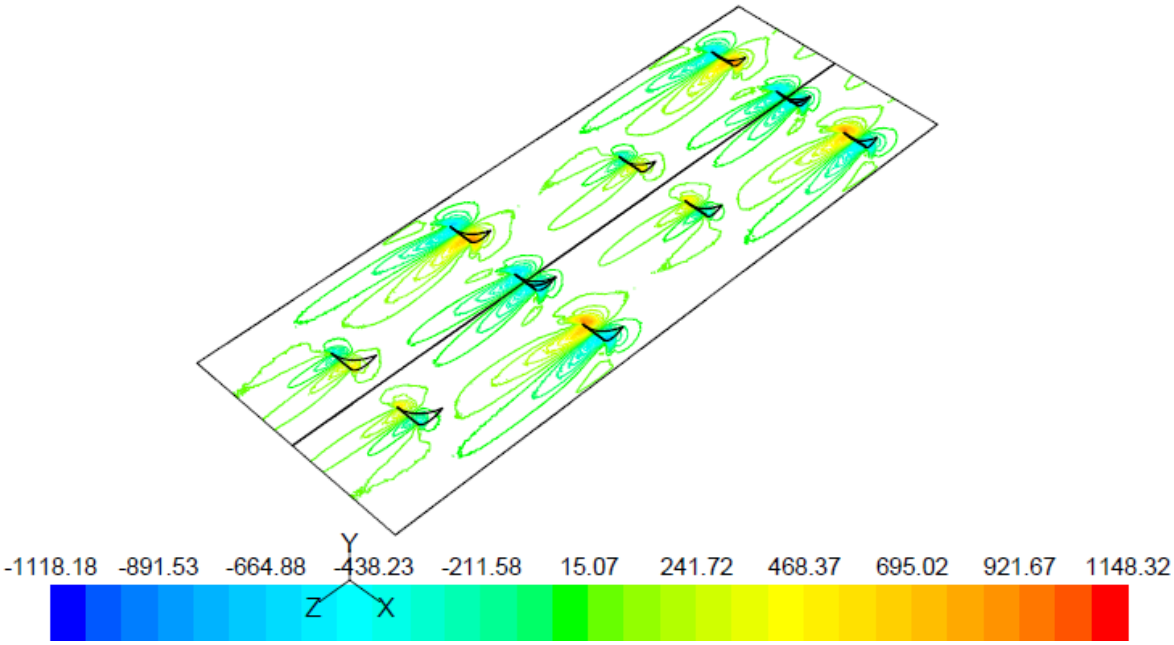

Fig. 21 Vorticity for P_t/b = 7/3, e/H = 0.50, P_l/e = 11/2, Re = 3000, α = 60° obstacles

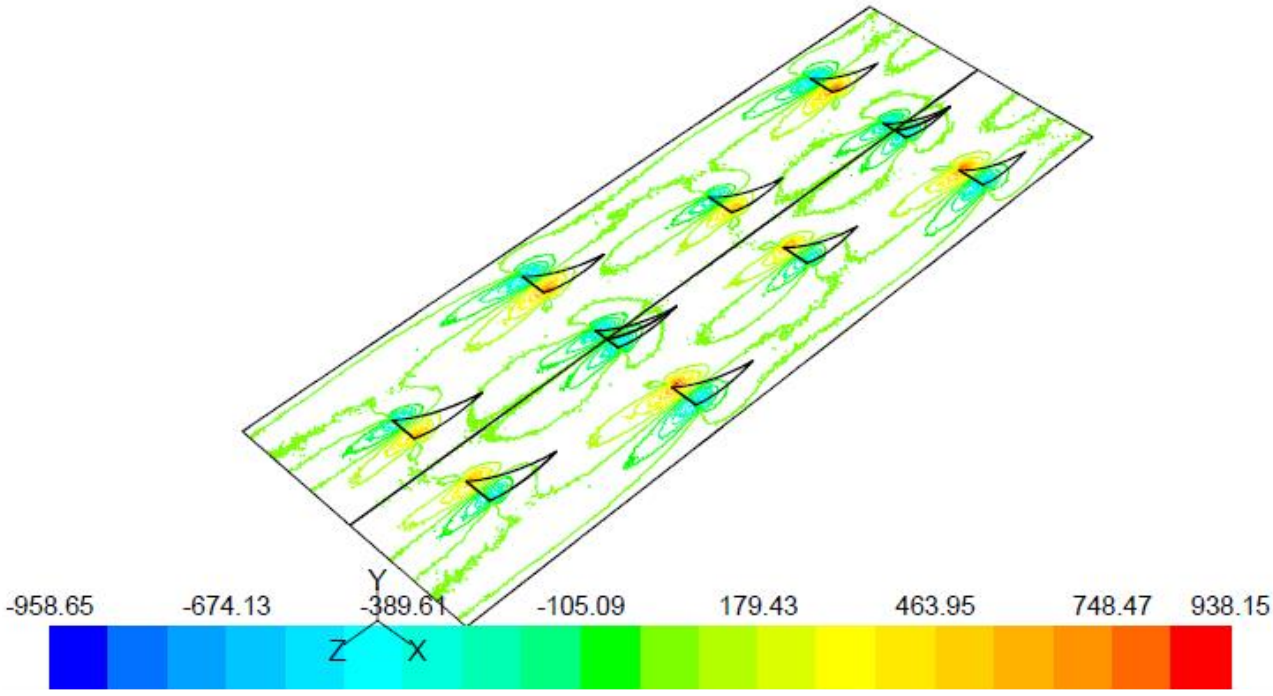

Fig. 22 Vorticity for P_t/b = 7/3, e/H = 0.50, P_l/e = 11/2, Re = 3000, α = 30° obstacles

The contour plots of the turbulence intensity caused by these vortices are shown in Figs. 23, 24 and 25 for angle of attack 90°, 60° and 30° respectively. From these figures it is observed that higher turbulence intensity is occurred just next to the obstacle for all angle of attacks. This

results in increase in convective heat transfer coefficient between the absorber plate and the air at this location.

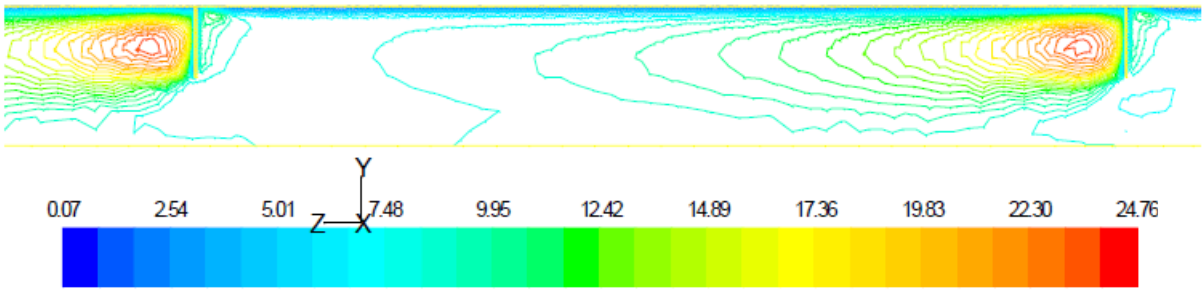

Fig. 23 Turbulent intensity for P_t/b = 7/3, e/H = 0.50, P_l/e = 11/2, Re = 3000, α = 90°obstacles

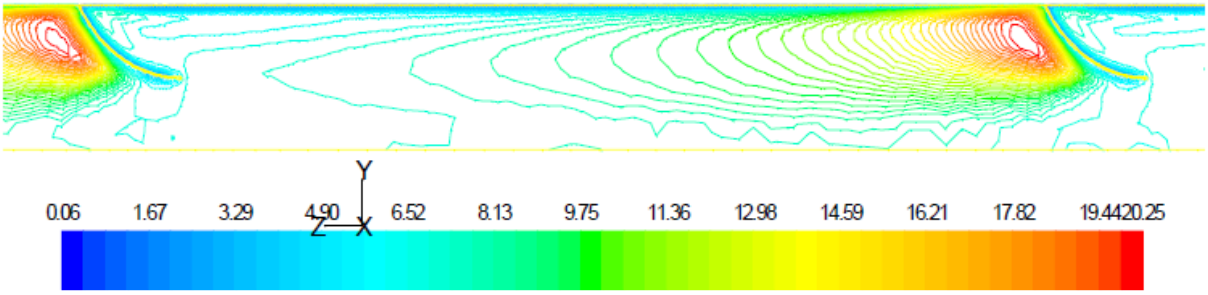

Fig. 24 Turbulent intensity for P_t/b = 7/3, e/H = 0.50, P_l/e = 11/2, Re = 3000, α = 60° obstacles

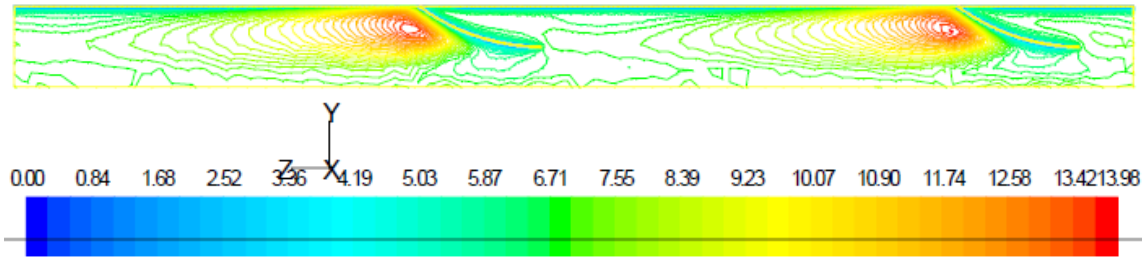

Fig. 25 Turbulent intensity for P_t/b = 7/3, e/H = 0.50, P_l/e = 11/2, Re = 3000, α = 30° obstacles

The contours of static temperature on the absorber plate presented in Figs. 26, 27, 28 show that the static temperature of the absorber plate next to the obstacles in the downstream direction is very low. This means more heat is lost from the absorber plate at this position and its temperature is lowered. This heat lost from the absorber plate is transferred to the flowing air.

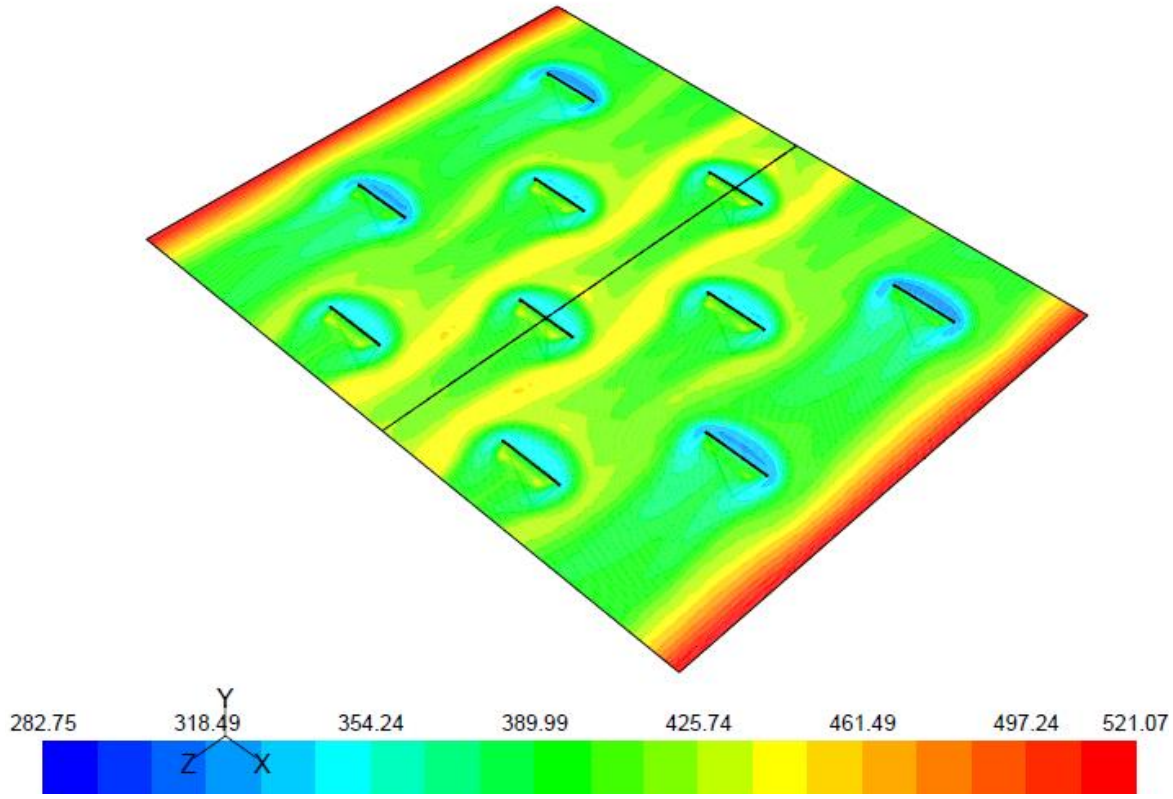

Fig. 26 Static temperature contours for P_l/e = 3/2, P_t/b = 7/3, e/H = 0.50, α = 90°°, Re = 3000

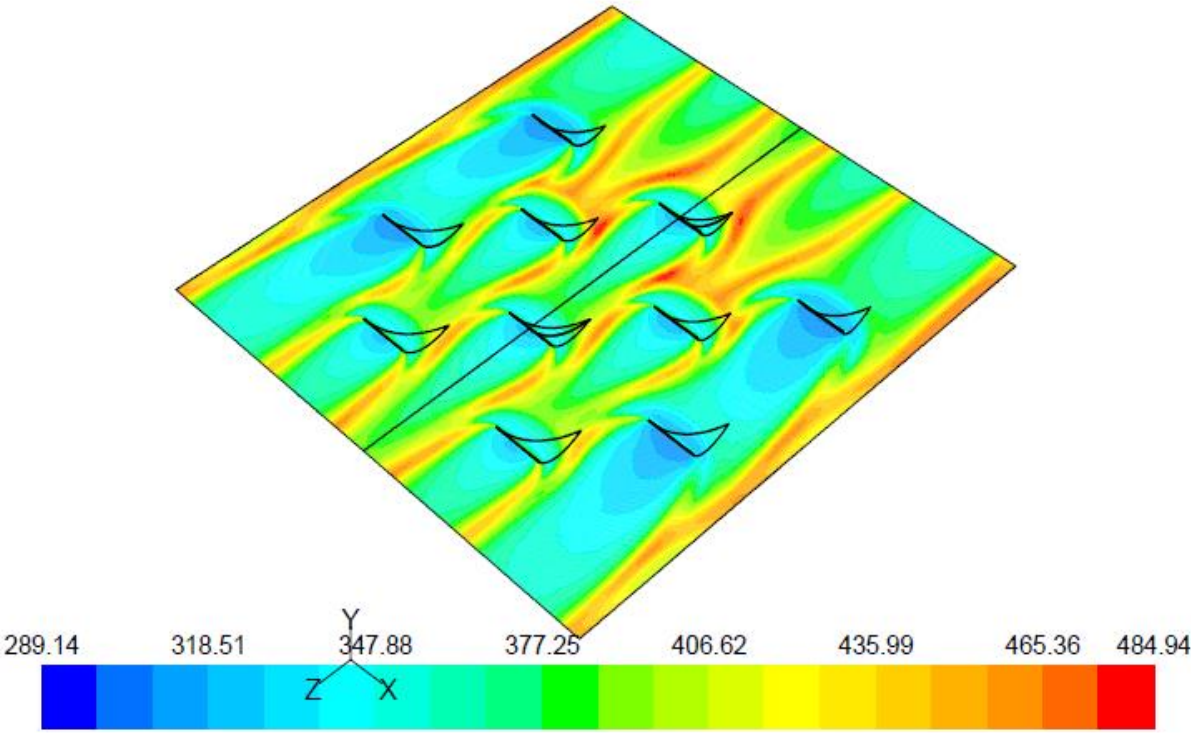

Fig. 27 Static temperature contours for P_l/e = 3/2, P_t/b = 7/3, e/H = 0.50, α = 60°, Re = 3000

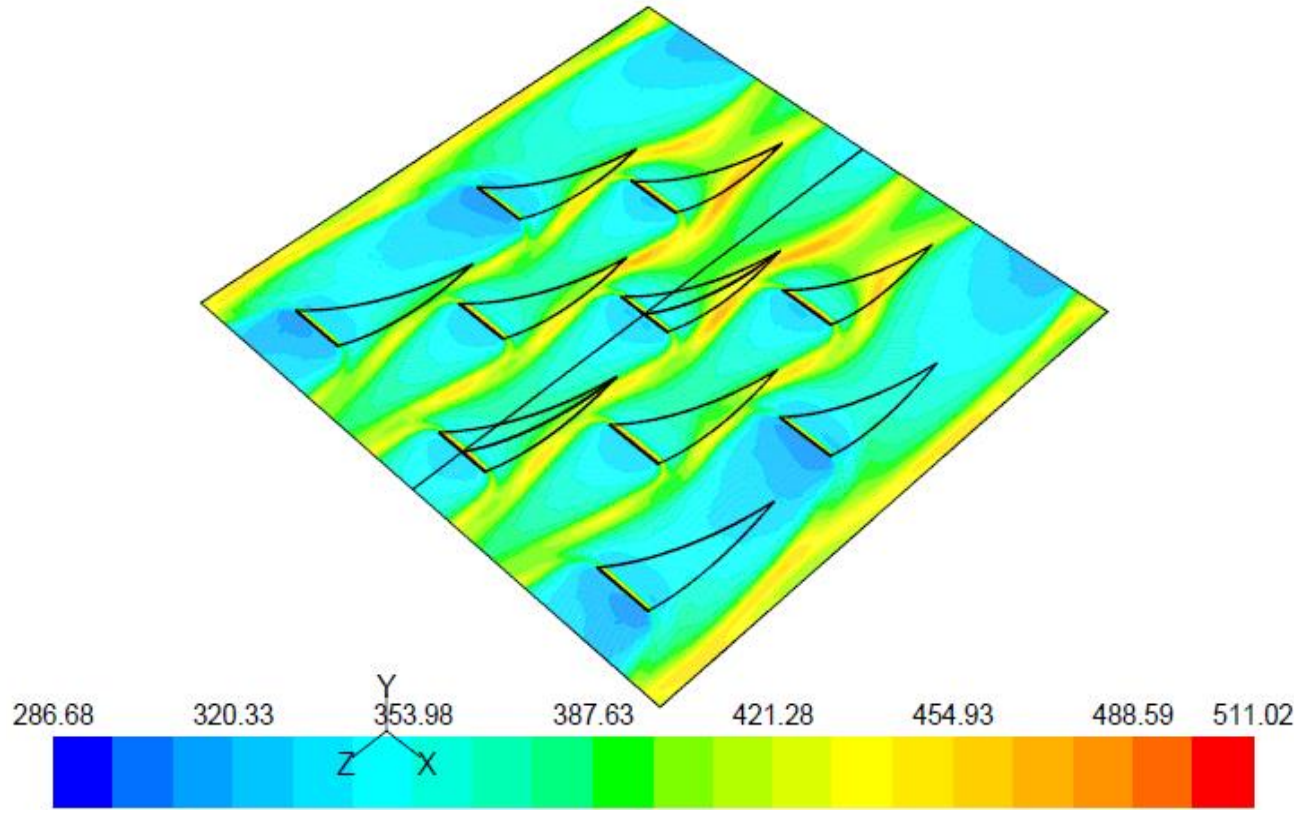

Fig. 28 Static temperature contours for P_l/e = 3/2, P_t/b = 7/3, e/H = 0.50, α = 30°, Re = 3000

The turbulence intensity along the length of the absorber (Fig. 29) passing through the obstacles shows the turbulence intensity is maximum next to the obstacle in downstream and get lowered as get far from the obstacle up to the next obstacle. Similarly, the convective heat transfer coefficient (Fig. 30) is maximum next to the obstacle in downstream direction.

As indicated earlier by previous studies, the longitudinal vortices (at angle of attack 60° and 30°) show higher turbulence intensity and better heat transfer characteristics than transverse vortices (at angle of attack 90°).

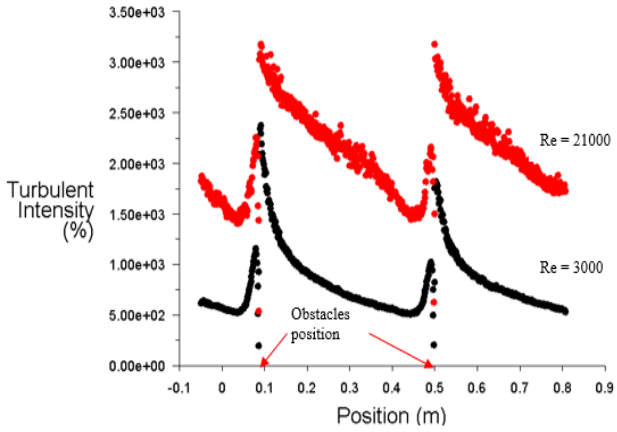

Fig. 29 Turbulent intensity along the obstacles for P_l/e = 11/2, P_t/b = 7/3, e/H = 0.50, α = 30°

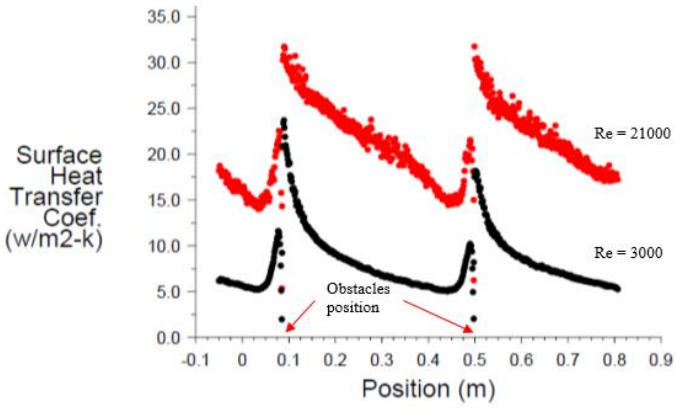

Fig. 30 Surface heat transfer coefficient along the obstacles for P_l/e = 11/2, P_t/b = 7/3, e/H = 0.50, α = 30 °

In this numerical study, the effect of obstacles arrangement have also been studied and the results for the maximum and minimum relative obstacles longitudinal pitch of the present study (P_l/e = 11/2 and P_l/e = 3/2) are presented. When the relative obstacles longitudinal pitch decreases to P_l/e = 3/2, since the space between obstacles decreases, the vortex generated will continue propagating up to the next obstacles. This will increase the turbulence intensity over the whole length between the obstacles causing heat transfer from larger space of absorber plate than the same in arrangement with larger relative obstacles longitudinal pitch of P_l/e = 11/2 in which the vortex generated die before reaching to the next obstacle. Thus, it has been observed that the turbulent intensity as well as the convective heat transfer is higher for lower relative obstacles longitudinal pitch.

The location of maximum heat transfer coefficient is seen at the location of the obstacles as the flow impinges on the surface of the obstacles. The heat transfer enhancement is most distractive around the obstacle area. In particular, the largest increase in the local heat transfer occurs on the obstacle followed by a sudden drop immediately after the obstacle and rapid recovery of the local heat transfer coefficient before facing the next obstacle.

4. 2 Experimental Result

Various tests have been conducted in order to obtain the optimum drying efficiency by varying tarbulators/ obstacles installation surface and flow condition.

With the optimum obstacle geometry (α = 60°) obtained via numerical study, the experimental set-up is prepared with three different obstacles configuration.

- Collector 1 (C1) – Smooth absorber plate collector
- Collector 2 (C2) - obstacles mounted on the absorber plate
- Collector 3 (C3) - obstacles mounted on the bottom plate

The absorber plate temperature distribution is measured with three thermocouples installed at different locations. These are:

- Tp1 – Temperature of absorber plate at the bottom
- Tp2 - Temperature of absorber plate at the middle
- Tp3 - Temperature of absorber plate at the top

Table 5 Sample test data of tomato

COLLECTOR-1 (without obstacles attached on the absorber plate)						
Time	Tp1	Tp2	Tp3	Tamb	To	Ibb
2:00	32	40	45	24	27	512
3:00	48	64	71	32	36	805
4:00	59	78	90	35	42	1029
5:00	66	90	102	39	46	1187
6:00	64	89	99	35	43	1198
7:00	62	86	95	33	42	1158
8:00	60	81	90	32	41	1050
9:00	55	71	79	31	40	806
10:00	45	57	61	30	37	316

COLLECTOR-2 (with obstacles attached on the absorber plate)						
Time	Tp1	Tp2	Tp3	Tamb	To	Ibb
2:00	33	37	40	24	32	543
3:00	45	53	58	32	43	830
4:00	51	62	70	35	50	1044
5:00	56	70	79	39	56	1189
6:00	54	67	76	35	53	1170
7:00	53	66	75	33	52	1150
8:00	52	64	73	32	51	1039
9:00	49	58	64	31	46	776
10:00	40	48	52	30	42	532

COLLECTOR-3 (with obstacles attached on the bottom plate)						
Time	Tp1	Tp2	Tp3	Tamb	To	Ibb
2:00	34	42	45	24	31	565
3:00	44	57	61	32	36	847
4:00	51	67	73	35	43	1067
5:00	58	75	83	39	47	1195
6:00	57	76	85	35	48	1244
7:00	55	74	84	33	46	1163
8:00	54	73	83	32	45	979
9:00	51	64	70	31	43	770
10:00	46	53	57	30	39	518

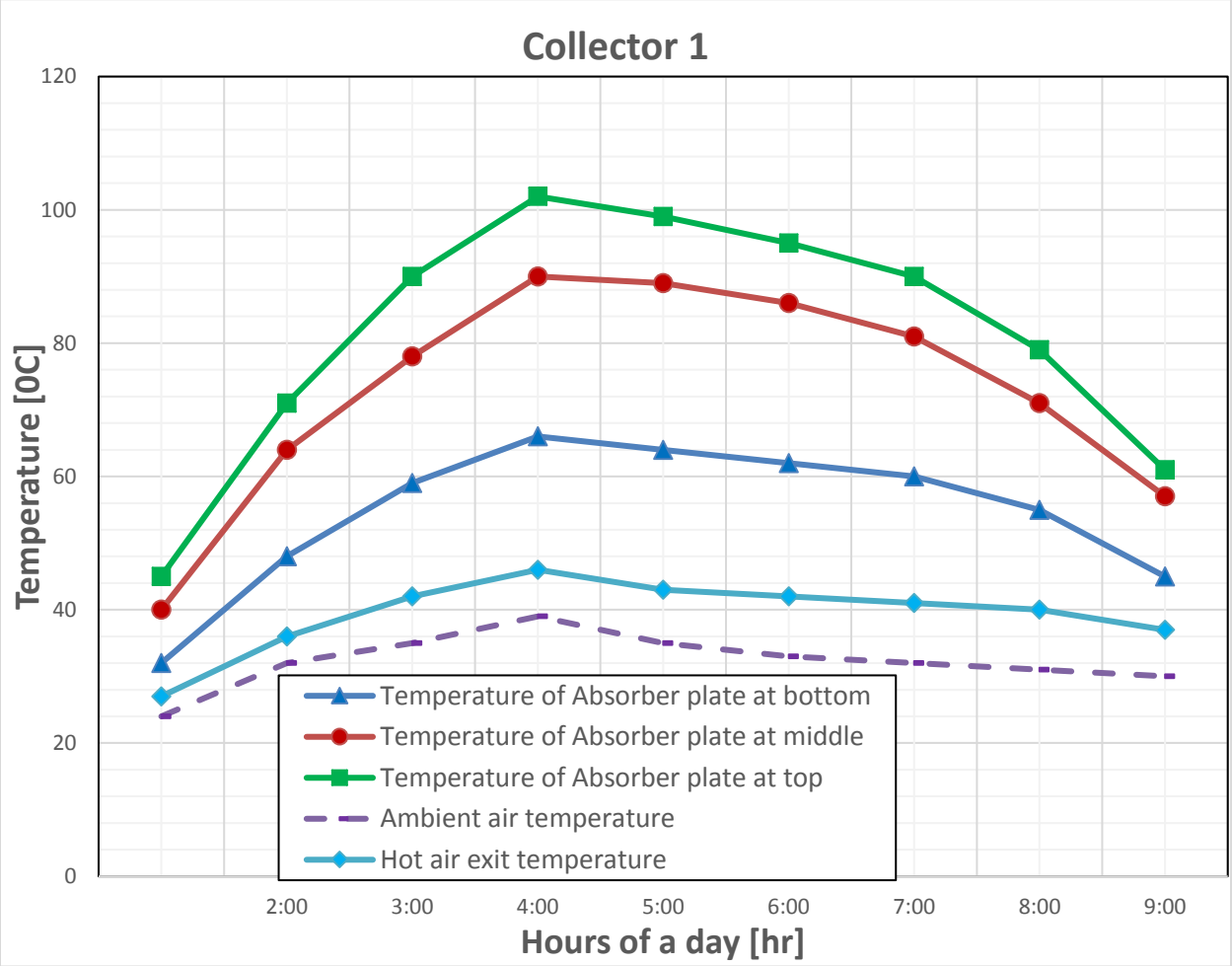

Fig. 31 Sample temperature plot of collector 1

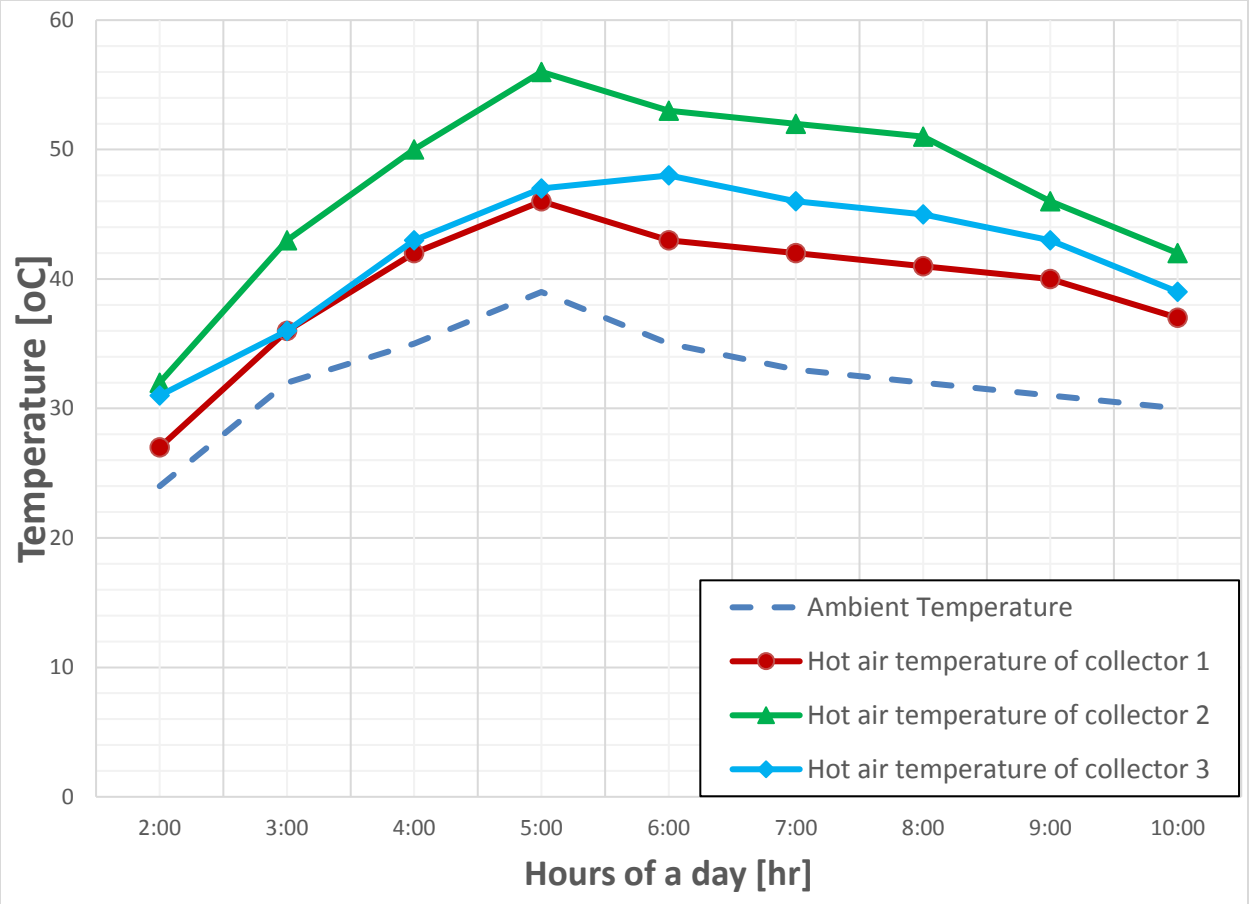

Fig. 32 Sample hot air temperature comparison

This test data shows that the temperature of the hot air obtained from collector - 2 is higher than that of collector – 3 which is again higher than collector – 1 which reflects the efficiency of the collectors. Thus the final dissemination of the solar drier is of type of arrangement 2.

a) Tomato drying

Table 6 Tomato drying data

Collector for tomato drying	**C1**	**C2**	**C3**
The initial weight of the tomato inserted in one drier	9.5 Kg	9.5 Kg	9.5 Kg
The Final weight of the tomato obtained from one drier	0.6 Kg	0.6 Kg	0.6 Kg
Moisture removed	93.68%	93.68%	93.68%
Drying time for tomato	3 days	3 days	3 days
Drying capacity of the drier	20 Kg	20 Kg	20 Kg

Fig. 33 Sample tomato test

b) Onion Drying

Table 7 Onion drying data

Collector for Onion drying	**C1**	**C2**	**C3**
The initial weight of the onion inserted in one drier	6.6 Kg	6.6 Kg	6.6 Kg
The Final weight of the onion obtained from one drier	5.5 Kg	5.5 Kg	5.5 Kg
Moisture removed	6.6 Kg	16.7 %	16.7 %
Drying time for onion	5.5 Kg	5 days	5 days
Drying capacity of the drier	20 Kg	20 Kg	20 Kg

Fig. 34 Onion after drying in solar drier

Fig. 35 Sample onion before drying (left) after drying (right)

c) Coffee Drying

The traditional way of coffee drying in Jimma zone, Haroo kebele is shown in the figure below. Here as it can be seen the coffee is drying in the sun near the road where the dust from the road whenever vehicle pass will cover the coffee and the coffee will be full of dust and different microorganisms will growth in the coffee and will make it of poor quality. It can also be seen that during the night time the coffee should be collected back to house and again back to the drying place during the day time this requires great labor work. It should also be noted that these coffees should be supervised by someone the whole day otherwise it can be stolen.

Fig. 36 Traditional way of coffee drying in Jimma Zone, Haroo Kebele

Even though coffee drying test is not done in the laboratory, the system is tested in Haroo kebele as shown in Fig 37 and it is found that it will solve all these problems by making less labor requirement, better quality coffee and less drying time. Hence the life of the farmers and the economy of the country will be improved by using this research outcome.

Fig. 37 Coffee drying test at Jimma Zone, Haroo kebele

5. Conclusions and Recommendations

5.1 Conclusion

The present research work is a numerical and experimental investigation of solar drier with delta-shaped obstacles mounted on the absorber plate.

A three dimensional CFD analysis of fluid flow and heat transfer characteristics in a rectangular duct having delta shaped obstacles mounted on one surface, has been done. The computational model of the present physical domain is developed using GAMBIT 2.4 and the analysis is carried out using ANSYS FLUENT 12.1 commercial software package. It is quite complex to construct and analyze the whole geometry of flow domain because of tremendous computational efforts required for this purpose. In order to accurately predict the result, the mesh near the obstacles should be very fine, thus a "fixed size function" is attached to all surfaces of the obstacles and to the absorber plate. Tetrahedral/Hybrid mesh element with T-Grid meshing scheme is used for meshing the model. By using CFD software flow and heat transfer behavior of the delta shaped obstacles of different arrangements have been investigated.

In this study three different experimental set-up, including one with smooth ducts and two with obstacles mounted on absorber plate and on the bottom wall, have been used to collect the experimental data. Data have been collected for temperature distribution on the heated plate, at inlet and outlet of the collector as a function of configuration of the delta-shaped obstacles for a given operating conditions.

Finally the following conclusions can be drawn from the present work:

- The heat transfer coefficient of delta-shaped obstacles mounted drier is found to increase with a decrease in relative obstacles longitudinal pitch (P_l/e), with a decrease in relative obstacles transversal pitch (P_t/b) and with an increase in the relative obstacles height (e/H) as expected.
- The optimum values of heat transfer coefficient are obtained at an angle of attack of 60°, and for P_l/e = 3/2, e/H = 0.75 when the obstacles are fixed on the absorber plate. This shows the benefit of bending the obstacles which helps to divert more fluid towards the heated plate and hence
- Solar drier made up metal gives higher performance due to the fact that the drying box is made of metal and painted black so that it absorbs additional solar radiation to the system.

- Solar drier with delta shaped obstacles mounted on the absorber surface gives better performance compared with the one fixed on the bottom wall and without obstacles
- The drying time and product quality obtained in drying tomato and onion are very impressive and will significantly solve the existing post-harvest and drying challenges.
- Drying coffee using this solar drier have been observed to significantly solve the drying quality, labor required, drying time and post-harvest loss.

5.2 Recommendations for future work

In the present work pressure drop and mas flow rate is not measured due to lack of instrument. Hence, it is suggested to study these parameters with appropriate instruments. Further research can be done with the same set-up to dry vegetables and fruits like; green paper, banana, mango, apple and etc.

Financial Expenditure

ITEMS	BUDGET GRANTED	BUDGET UTILIZED
Personal: • Data Collection (Input data) • Design of the system (Component Design with detail drawing for manufacturing)	• 66,200.00	66,058.00
Local travel: • Vehicle & related • Fuel • Repair	• 11,000.00	15,500.00
Field Substances • Per diem for Sample distribution for farmer, installation, test and train the user	• 4,500.00	-
Services: • Workshop (man power for manufacturing)	• 15,960.00	15,878.36
Equipment:	165,120.00	43,734.57
Total	**262,780.00**	**141,170.93**

References

Abene, A., Dubois, V., Le Ray, M., Ouagued, A. (2004). Study of a Solar Air Flat Plate Collector: Use of Obstacles and Application for the Drying of Grape. Journal of Food Engineering, 65: 15–22.

Adisu Bekele, Manish Mishra & Sushanta Dutta, (2011). "Heat transfer augmentation in solar air heater using delta-shaped obstacles mounted on the absorber plate". *International Journal of Sustainable Energy, 32:1, 53-69.*

Alvarez, G., Arce, J., Lira, L., Heras, M. R. (2004). Thermal Performance of An Air Solar Collector with an Absorber Plate Made of Recyclable Aluminum Cans. Solar Energy, 77(1):107–113.

Ben Slama, R. (2007). The Air Solar Collectors: Comparative Study, Introduction of Baffles to Favor the Heat Transfer. Solar Energy, 81: 139 – 149.

Esen, H. (2008). Experimental Energy and Exergy Analysis of a Double-Flow Solar Air Heater Having Different Obstacles on Absorber Plates. Building and Environment, 43: 1046–1054.

Gbaha, P. (1989). Study and Optimization of Heat Exchange and Performances of the Plane Solar Collectors with Two Air Veins. Thesis of speciality in energetics, Universite´ de Valenciennes, France, February.

Hachemi, A. (1992). Contribution to obtaining the thermal performances of the plane solar air colectors, at bed furnished with lines of obstacles with tight steps. *Doctorate thesis, University of Valenciennes, France.*

Moummi, A. (1994). General and local study of the geometry role in the optimization of the air solar collectors. Thesis of speciality in energetics, University of Valenciennes, France.

Moummi, N. (1995). Pre´visions syste´matiques et optimization des performances des capteurs solaires plans a` air dans divers sites de climates me´diterrane´ens ou sahaliens avec ou sans altitude. Thesis of speciality in energetics, University of Valenciennes, France.

Moummi, N., Ali, S. Y., Moummi, A., Desmons, J. Y. (2004). Energy Analysis of a Solar Air Collector with Rows of Fins. Renewable Energy, 29(13): 2053–64.

Ozgen, F., Esen, M., Esen, H. (2009). Experimental Investigation of Thermal Performance of a Double-Flow Solar Air Heater Having Aluminium Cans. Renewable Energy, 34: 2391–2398.

Annex A: Picture of Dissemination of the Research Outcome to the beneficiaries

Fig. 38: products ready for dissemination

Fig. 39: Dissemination in east Showa zone, Bekele Girrisa kebele

Fig. 40: Dissemination in Jimma Zone, Haroo kebele

Fig. 41: Dissemination at Fogera woreda Woreta city under AgroBig Project

Annex B: Tomato Drying Test Data at different Time

	COLLECTOR-1						10-01-15
Time	Tp1	Tp2	Tp3	To	Tamb	Ibb	
2:00							
3:00							
4:00							
5:00							
6:00							
7:00	64	88	96	46			
8:00	63	84	91	43			
9:00	58	72	78	40			
10:00	47	59	63	36			
11:00	32	34	36	31			

	COLLECTOR-2						10-01-15
Time	Tp1	Tp2	Tp3	To	Tamb	Ibb	
2:00							
3:00							
4:00							
5:00							
6:00							
7:00	57	68	76	52			

8:00	54	64	71	51			
9:00	50	58	64	47			
10:00	44	49	53	42			
11:00	35	34	35	33			

	COLLECTOR-3						10-01-15
Time	Tp1	Tp2	Tp3	To	Tamb	Ibb	
2:00							
3:00							
4:00							
5:00							
6:00							
7:00	59	79	87	50			
8:00	60	75	81	48			
9:00	51	65	70	42			
10:00	44	54	57	38			
11:00	30	32	34	30			

	COLLECTOR-1							10-02-15
Time	Tp1	Tp2	Tp3	To	Tamb	Ibb		
2:00	29	38	41	21	23			
3:00	45	58	64	30	33			
4:00	54	72	81	36	32			
5:00	62	82	90	41	37			
6:00	56	79	88	38	34			
7:00	62	84	93	40	42			
8:00	57	77	84	39	41			
9:00	54	70	77	37	41			
10:00	46	56	61	35	31			

	COLLECTOR-2						10-02-15
Time	Tp1	Tp2	Tp3	To	Tamb	Ibb	
2:00	30	33	36	27			
3:00	41	47	52	37			

4:00	46	57	63	45			
5:00	45	56	65	48			
6:00	52	63	71	48			
7:00	54	65	73	51			
8:00	50	60	67	48			
9:00	47	55	61	45			
10:00	45	49	52	41			

	COLLECTOR-3						10-02-15
Time	Tp1	Tp2	Tp3	To	Tamb	Ibb	
2:00	30	37	39	26			
3:00	37	50	53	31			
4:00	42	61	67	41			
5:00	46	60	63	36			
6:00	51	71	79	43			
7:00	53	75	83	47			
8:00	52	72	76	44			
9:00	51	63	68	41			
10:00	43	51	54	37			

	COLLECTOR-1							10-03-15
Time	Tp1	Tp2	Tp3	To	Tamb	Ibb		
2:00	27	37	41	21	19			
3:00	41	56	62	30	25			
4:00	51	71	38	37	31			
5:00	60	84	93	42	36			
6:00	60	83	92	41	36			
7:00	58	81	89	39	28			
8:00	56	75	83	38	32			
9:00	55	72	77	39	34			
10:00	38	42	45	32	31			

	COLLECTOR-2						10-03-15
Time	Tp1	Tp2	Tp3	To	Tamb	Ibb	
2:00	28	33	36	27	19		
3:00	39	47	51	37	25		
4:00	47	57	64	45	31		
5:00	53	64	73	53	36		
6:00	51	64	72	49	36		
7:00	48	62	70	49	28		
8:00	49	61	68	48	32		
9:00	46	52	58	45	34		
10:00	36	38	39	35	31		

	COLLECTOR-3						10-03-15
Time	Tp1	Tp2	Tp3	To	Tamb	Ibb	
2:00	31	41	42	27	19		
3:00	36	48	52	30	25		
4:00	41	59	65	36	31		
5:00	48	68	75	41	36		
6:00	52	72	80	44	36		
7:00	51	72	80	45	28		
8:00	51	71	77	45	32		
9:00	48	61	65	41	34		
10:00	35	37	39	31	31		

	COLLECTOR-1							10-04-15
Time	Tp1	Tp2	Tp3	To	Tamb	Ibb		
2:00	29	39	44	21	20			
3:00	48	64	72	33	29			
4:00	54	73	82	37	33			
5:00	63	84	93	41	36			
6:00	63	88	97	40	36			

7:00	48	59	63	36	32			
8:00	36	40	42	30	30			
9:00	38	43	45	31	30			
10:00	34	38	39	29	28			

	COLLECTOR-2						10-04-15
Time	Tp1	Tp2	Tp3	To	Tamb	Ibb	
2:00	27	32	35	25	20		
3:00	41	51	56	40	29		
4:00	48	61	67	46	33		
5:00	51	64	71	48	36		
6:00	52	64	72	49	36		
7:00	42	46	50	38	32		
8:00	33	34	36	32	30		
9:00	34	36	37	33	30		
10:00	32	31	32	30	28		

	COLLECTOR-3						10-04-15
Time	Tp1	Tp2	Tp3	To	Tamb	Ibb	
2:00	35	42	43	29	20		
3:00	43	55	58	34	29		
4:00	53	68	73	42	33		
5:00	54	64	66	40	36		
6:00	57	80	89	48	36		
7:00	45	54	56	39	32		
8:00	37	38	39	32	30		
9:00	38	41	42	33	30		
10:00	34	35	35	30	28		

COLLECTOR-1(cloudy day)							10-05-15
Time	Tp1	Tp2	Tp3	To	Tamb	Ibb	
2:00	26	31	33	23	23		
3:00	34	39	41	26	25		
4:00	54	70	78	36	33		
5:00	50	64	70	35	33		
6:00	52	67	74	36	34		
7:00	55	71	77	38	33		
8:00	46	56	60	35	32		
9:00	40	46	47	33	30		
10:00							

COLLECTOR-2(Cloudy day)							10-05-15
Time	Tp1	Tp2	Tp3	To	Tamb	Ibb	
2:00	27	28	29	24	23		
3:00	29	30	32	26	25		
4:00	44	49	53	41	33		
5:00	45	49	52	40	33		
6:00	45	51	56	42	34		
7:00	48	52	57	44	33		
8:00	45	48	50	41	32		
9:00	35	37	39	35	30		There are no items(tomato)
10:00							

COLLECTER-3 (Cloudy day) 05/10/2015							10-05-15
Time	Tp1	Tp2	Tp3	To	Tamb	Ibb	
2:00	30	33	33	26	23		
3:00	35	37	39	29	25		
4:00	47	55	57	37	33		
5:00	50	59	63	40	33		
6:00	53	69	73	45	34		Fan is not working
7:00	61	79	83	54	33		
8:00	53	62	65	46	32		
9:00	44	49	50	41	30		
10:00							

COLLECTOR-1							10-12-15
Time	Tp1	Tp2	Tp3	Tamb	To	Ibb	Remark
4:00	61	85	97		46	990	
5:00	76	106	113		58	1118	
6:00	77	107	113	35	60	1171	
7:00	74	103	108	31	56	1129	
8:00	75	103	108	32	57	1014	
9:00	66	87	91	31	55	768	
10:00	55	69	74	25	48	513	

COLLECTOR-2							10-12-15
Time	Tp1	Tp2	Tp3	Tamb	To	Ibb	Remark
4:00	56	65	73		52	1009	
5:00	60	72	79		56	1130	
6:00	55	67	75		57	1179	
7:00	55	67	75		53	1143	
8:00	54	65	74		54	1024	
9:00	50	56	64		48	763	
10:00	45	49	53		42	523	

COLLECTOR-3							10-12-15
Time	Tp1	Tp2	Tp3	Tamb	To	Ibb	Remark
4:00	54	70	77		43	1019	
5:00	56	75	82		45	1142	
6:00	55	77	86		47	1188	
7:00	63	82	91		51	1140	
8:00	58	77	85		50	964	
9:00	51	65	70		44	751	
10:00	45	52	57		39	521	

COLLECTOR-1							13/10/2015
Time	Tp1	Tp2	Tp3	Tamb	To	Ibb	Remark
2:00	30	40	45	20	22	510	
3:00	53	68	77	34	38	815	
4:00	61	80	93	38	43	1059	
5:00	68	91	102	37	47	1184	
6:00	66	91	102	35	46	1214	
7:00	63	87	96	32	43	1150	
8:00	68	89	98	37	46	1026	
9:00	56	72	78	34	41	804	
10:00	47	59	63	32	38	640	

COLLECTOR-2							13/10/2015
Time	Tp1	Tp2	Tp3	Tamb	To	Ibb	Remark
2:00	31	35	38	20	30	524	
3:00	47	56	61	34	45	833	
4:00	53	63	72	38	52	1070	
5:00	60	70	80	37	57	1194	
6:00	61	72	80	35	59	1239	
7:00	56	68	76	32	53	1179	
8:00	60	71	78	37	55	1009	
9:00	50	59	65	34	49	809	
10:00	45	49	54	32	43	548	

COLLECTOR-3							13/10/2015
Time	Tp1	Tp2	Tp3	Tamb	To	Ibb	Remark
2:00	46	53	55	20	40	562	
3:00	48	59	63	34	37	860	
4:00	53	69	76	38	44	1103	
5:00	58	76	83	37	47	1190	
6:00	62	80	88	35	50	1247	
7:00	57	76	85	32	48	1186	
8:00	62	78	87	37	52	980	
9:00	52	66	72	34	45	791	
10:00	44	51	56	32	38	530	

COLLECTOR-1							14/10/2015
Time	Tp1	Tp2	Tp3	Tamb	To	Ibb	Remark
2:00	32	40	45	24	27	512	
3:00	48	64	71	32	36	805	
4:00	59	78	90	35	42	1029	
5:00	66	90	102	39	46	1187	
6:00	64	89	99	35	43	1198	
7:00	62	86	95	33	42	1158	
8:00	60	81	90	32	41	1050	
9:00	55	71	79	31	40	806	
10:00	45	57	61	30	37	316	

COLLECTOR-2							14/10/2015
Time	Tp1	Tp2	Tp3	Tamb	To	Ibb	Remark
2:00	33	37	40	24	32	543	
3:00	45	53	58	32	43	830	
4:00	51	62	70	35	50	1044	
5:00	56	70	79	39	56	1189	
6:00	54	67	76	35	53	1170	
7:00	53	66	75	33	52	1150	
8:00	52	64	73	32	51	1039	
9:00	49	58	64	31	46	776	
10:00	40	48	52	30	42	532	

COLLECTOR-3							14/10/2015
Time	Tp1	Tp2	Tp3	Tamb	To	Ibb	Remark
2:00	34	42	45	24	31	565	
3:00	44	57	61	32	36	847	
4:00	51	67	73	35	43	1067	
5:00	58	75	83	39	47	1195	
6:00	57	76	85	35	48	1244	
7:00	55	74	84	33	46	1163	
8:00	54	73	83	32	45	979	
9:00	51	64	70	31	43		
10:00	46	53	57	30	39	518	

COLLECTOR-1							15/10/2015
Time	Tp1	Tp2	Tp3	Tamb	To	Ibb	Remark
2:00	32	42	48	23	24	530	
3:00	38	45	49	27	28	375	cloudy
4:00	55	73	82	34	39	1009	
5:00	63	86	98	38	46	1167	
6:00	61	86	95	36	42	1230	
7:00	61	85	94	32	42	1225	
8:00	56	78	87	31	41	1090	
9:00	46	60	70	30	38	909	
10:00	44	56	60	30	36	316	

COLLECTOR-2							15/10/2015
Time	Tp1	Tp2	Tp3	Tamb	To	Ibb	Remark
2:00	34	39	43	23	33	565	
3:00	35	39	41	27	33	435	cloudy
4:00	48	59	66	34	49	932	
5:00	55	69	78	38	55	1189	
6:00	53	68	76	36	53	1237	
7:00	53	68	76	32	53	1220	
8:00	50	58	66	31	50	1118	
9:00	46	52	68	30	44	809	
10:00	42	48	53	30	41	636	

COLLECTOR-3							15/10/2015
Time	Tp1	Tp2	Tp3	Tamb	To	Ibb	Remark
2:00	45	51	54	23	37	577	
3:00	39	43	45	27	31	499	cloudy
4:00	42	59	66	34	38	1040	
5:00	52	72	80	38	45	1193	
6:00	53	74	83	36	46	1238	
7:00	54	76	84	32	47	1211	
8:00	50	69	77	31	44	1121	
9:00	46	58	59	30	40	801	
10:00	42	51	56	30	38	636	

Annex C: Onion Drying Test Data at different Time

COLLECTOR-1							19/10/2015
Time	Tp1	Tp2	Tp3	Tamb	To	Ibb	Remark
2:00							
3:00							
4:00							
5:00	38	48	54	26	30		
6:00	53	76	87	30	35		Unstable weather condition
7:00	41	50	55	28	32		
8:00	49	66	71	32	34		
9:00	51	68	74	32	35		
10:00	42	55	62	28	33		

COLLECTOR-2							19/10/2015
Time	Tp1	Tp2	Tp3	Tamb	To	Ibb	Remark
2:00							
3:00							
4:00							
5:00	35	40	44	26	35		
6:00	47	56	64	30	45		Unstable weather condition
7:00	38	40	43	28	36		
8:00	44	57	64	32	45		
9:00	40	55	62	32	44		
10:00	38	49	55	28	42		

COLLECTOR-3							19/10/2015
Time	Tp1	Tp2	Tp3	Tamb	To	Ibb	Remark
2:00							
3:00							
4:00							
5:00	37	52	57	26	32		
6:00	47	62	71	30	41		Unstable weather condition
7:00	40	43	45	28	32		
8:00	46	64	70	32	42		
9:00	45	61	66	32	39		

10:00	42	54	58	28	36		

COLLECTOR-1							20/10/2015
Time	Tp1	Tp2	Tp3	Tamb	To	Ibb	Remark
2:00	28	39	45	20	22		
3:00	42	58	66	27	30		
4:00	53	74	84	30	36		
5:00	61	87	98	36	42		
6:00	63	88	99	37	41		
7:00	50	70	79	32	37		cloudy
8:00	56	76	83	34	39		
9:00	49	67	73	33	37		
10:00	42	50	58	29	33		

COLLECTOR-2							20/10/2015
Time	Tp1	Tp2	Tp3	Tamb	To	Ibb	Remark
2:00	29	36	40	20	29		
3:00	40	50	55	27	39		
4:00	46	57	65	30	47		
5:00	53	67	77	36	53		
6:00	53	68	78	37	53		
7:00	47	53	59	32	44		cloudy
8:00	50	60	67	34	47		
9:00	46	56	62	33	44		
10:00	40	46	51	29	40		

COLLECTOR-3							20/10/2015
Time	Tp1	Tp2	Tp3	Tamb	To	Ibb	Remark
2:00	27	35	38	20	22		
3:00	37	47	51	27	30		
4:00	42	62	69	30	37		
5:00	49	69	78	36	40		
6:00	51	74	84	37	44		
7:00	45	60	66	32	41		cloudy
8:00	52	69	75	34	44		
9:00	48	62	67	33	41		
10:00	41	50	54	29	36		

COLLECTOR-1							21/10/2015
Time	Tp1	Tp2	Tp3	Tamb	To	Ibb	Remark
2:00	26	35	39	19	20		
3:00	44	60	68	28	32		
4:00	55	74	86	32	38		
5:00	63	88	100	37	42		
6:00	53	76	88	34	39		Cloudy
7:00	58	83	94	35	41		
8:00	55	78	85	34	40		
9:00							
10:00	45	53	60	30	35		

COLLECTOR-2							21/10/2015
Time	Tp1	Tp2	Tp3	Tamb	To	Ibb	Remark
2:00	27	33	36	19	27		
3:00	39	49	57	28	41		
4:00	48	60	70	32	50		
5:00	54	69	79	37	56		
6:00	48	53	73	34	50		Cloudy
7:00	52	67	77	35	52		
8:00	49	62	71	34	49		
9:00							
10:00	40	47	53	30	41		

COLLECTOR-3							21/10/2015
Time	Tp1	Tp2	Tp3	Tamb	To	Ibb	Remark
2:00	31	37	39	19	26		
3:00	37	50	55	28	31		
4:00	44	62	68	32	36		
5:00	51	72	80	37	42		
6:00	50	71	80	34	42		Cloudy
7:00	54	75	85	35	46		
8:00	53	73	81	34	41		
9:00							
10:00	42	51	55	30	37		

COLLECTOR-1							22/10/2015
Time	Tp1	Tp2	Tp3	Tamb	To	Ibb	Remark
2:00							
3:00	36	45	50	26	28		
4:00	40	54	63	29	33		
5:00	60	85	96	34	42		
6:00	66	89	99	35	43		
7:00	58	83	92	32	39		
8:00	56	77	87	31	38		
9:00	49	65	72	30	37		
10:00	43	52	59	28	34		

COLLECTOR-2							22/10/2015
Time	Tp1	Tp2	Tp3	Tamb	To	Ibb	Remark
2:00							
3:00	37	41	46	26	36		
4:00	43	52	60	29	43		
5:00	55	71	81	34	54		
6:00	54	69	79	35	54		
7:00	52	67	76	32	53		
8:00	50	62	70	31	48		
9:00	44	53	60	30	44		
10:00	41	46	51	28	40		

COLLECTOR-3							22/10/2015
Time	Tp1	Tp2	Tp3	Tamb	To	Ibb	Remark
2:00							
3:00	34	41	43	26	28		
4:00	41	55	60	29	34		
5:00	43	64	74	34	38		
6:00	53	77	83	35	43		
7:00	54	78	86	32	48		
8:00	51	69	77	31	44		
9:00	46	59	65	30	41		
10:00	41	50	54	28	36		

COLLECTOR-1	23/10/2010

Time	Tp1	Tp2	Tp3	Tamb	To	Ibb	Remark
2:00	28	36	40	20	22		
3:00	44	59	66	29	32		
4:00	49	66	75	30	34		
5:00	50	69	77	32	37		Unstable weather condition
6:00	61	86	97	34	41		
7:00	52	70	80	32	38		
8:00	58	81	91	34	40		
9:00							
10:00							

COLLECTOR-2							23/10/2015
Time	Tp1	Tp2	Tp3	Tamb	To	Ibb	Remark
2:00	28	34	37	20	29		
3:00	41	50	57	29	42		
4:00	40	47	53	30	40		
5:00	47	64	77	32	53		Unstable weather condition
6:00	53	69	79	34	54		
7:00	48	61	70	32	50		
8:00	52	66	76	34	53		
9:00							
10:00							

COLLECTOR-3							23/10/2015
Time	Tp1	Tp2	Tp3	Tamb	To	Ibb	Remark
2:00	36	44	46	20		32	
3:00	38	51	56	29		33	
4:00	37	47	52	30		32	
5:00	51	72	80	32		42	Unstable weather condition
6:00	55	76	85	34		45	
7:00	50	70	78	32		43	
8:00	58	77	86	34		49	
9:00							
10:00							

COLLECTOR-1							24/10/2015
Time	Tp1	Tp2	Tp3	Tamb	To	Ibb	Remark

2:00							
3:00							
4:00	58	78	90	32	39		
5:00	62	86	96	34	43		
6:00	59	84	95	33	40		
7:00	61	87	99	33	41		
8:00	64	90	89	34	44		
9:00	50	68	76	31	38		
10:00	42	52	57	29	35		

COLLECTOR-2							24/10/2015
Time	Tp1	Tp2	Tp3	Tamb	To	Ibb	Remark
2:00							I Can not take
3:00							
4:00	47	62	71	32	49		
5:00	52	67	77	34	53		
6:00	50	65	76	33	50		
7:00	52	68	78	33	53		
8:00	58	73	81	34	56		
9:00	43	52	62	31	47		
10:00	39	43	48	29	38		

COLLECTOR-3							24/10/2015
Time	Tp1	Tp2	Tp3	Tamb	To	Ibb	Remark
2:00							
3:00							
4:00	48	68	73	32	41		
5:00	52	73	81	34	43		
6:00	52	76	85	33	46		
7:00	57	79	88	33	48		
8:00	61	81	90	34	51		
9:00	49	63	70	31	43		
10:00	41	49	53	29	37		

COLLECTOR-1							25/10/2015
Time	Tp1	Tp2	Tp3	Tamb	To	Ibb	Remark

2:00	27	35	37	21	22		Very Cloudy day
3:00	26	30	31	21	22		
4:00	32	39	41	24	26		
5:00	38	46	49	27	29		
6:00	44	58	63	29	33		
7:00	49	64	71	32	37		
8:00	51	68	76	33	38		
9:00	43	53	58	31	36		
10:00	38	43	47	29	32		

COLLECTOR-2							25/10/2015
Time	Tp1	Tp2	Tp3	Tamb	To	Ibb	Remark
2:00	27	31	35	21	27		Very Cloudy day
3:00	26	27	29	21	25		
4:00	30	33	35	24	28		
5:00	35	39	42	27	33		
6:00	40	47	51	29	39		
7:00	44	50	56	32	42		
8:00	45	53	59	33	44		
9:00	39	41	45	31	38		
10:00	35	38	42	29	35		

COLLECTOR-3							25/10/2015
Time	Tp1	Tp2	Tp3	Tamb	To	Ibb	Remark
2:00	33	36	41	21	29		Very Cloudy day
3:00	29	32	33	21	26		
4:00	32	35	38	24	28		
5:00	37	44	46	27	32		
6:00	43	52	56	29	37		
7:00	46	57	61	32	40		
8:00	48	61	67	33	43		
9:00	41	46	50	31	36		
10:00	38	43	46	29	34		

COLLECTOR-1							26/10/2015
Time	Tp1	Tp2	Tp3	Tamb	To	Ibb	Remark

2:00	30	40	46	22	23		
3:00	48	65	76	32	35		
4:00	61	82	93	33	42		
5:00	64	90	102	34	45		
6:00	66	92	104	35	46		
7:00	60	85	97	32	39		
8:00	59	83	94	31	39		
9:00	54	74	82	30	38		
10:00	42	50	54	29	35		

COLLECTOR-2							26/10/2015
Time	Tp1	Tp2	Tp3	Tamb	To	Ibb	Remark
2:00	30	36	40	22	31		
3:00	44	54	62	32	44		
4:00	50	63	74	33	53		
5:00	55	70	80	34	57		
6:00	57	72	82	35	58		
7:00	51	66	77	32	53		
8:00	50	65	76	31	52		
9:00	46	54	66	30	49		
10:00	41	46	50	29	41		

COLLECTOR-3							26/10/2015
Time	Tp1	Tp2	Tp3	Tamb	To	Ibb	Remark
2:00	38	48	51	22	35		
3:00	46	57	63	32	38		
4:00	52	70	77	33	44		
5:00	55	75	84	34	46		
6:00	58	80	90	35	49		
7:00	57	79	89	32	48		
8:00	57	80	90	31	49		
9:00	51	69	75	30	47		
10:00	44	53	58	29	39		

COLLECTOR-1							27/10/2015
Time	Tp1	Tp2	Tp3	Tamb	To	Ibb	Remark

2:00	30	41	46	22	23		
3:00	49	65	75	31	37		
4:00	57	77	88	32	40		
5:00	65	89	99	36	44		
6:00	63	88	99	33	41		
7:00	61	86	98	32	40		
8:00	59	80	91	31	39		
9:00	52	69	76	30	38		
10:00							

COLLECTOR-2							27/10/2015
Time	Tp1	Tp2	Tp3	Tamb	To	Ibb	Remark
2:00	24	36	41	22	31		
3:00	44	54	61	31	46		
4:00	48	58	68	32	48		
5:00	55	67	81	36	56		
6:00	53	66	78	33	52		
7:00	52	66	78	32	52		
8:00	50	64	74	31	51		
9:00	44	50	61	30	46		
10:00							

COLLECTOR-3							27/10/2015
Time	Tp1	Tp2	Tp3	Tamb	To	Ibb	Remark
2:00	42	46	52	22	36		
3:00	44	56	61	31	37		
4:00	50	66	73	32	43		
5:00	55	76	84	36	46		
6:00	56	77	86	33	47		
7:00	58	79	88	32	50		
8:00	58	78	87	31	50		
9:00	50	65	71	30	45		
10:00							

I CERTIFY THAT THE INFORMATION AND FIGURES GIVEN IN THE REPORT ARE CORRECT AND COMPLETE TO THE BEST OF MY KNOWLEDGE.

SIGNATURE OF THE PRINCIPAL INNITITOR DATE

_____ _____

APPROVED BY THE HEAD OF THE DEPARTMENT DATE

NAME & SIGNATURE:_____ _____

APPROVED BY THE SCHOOL DATE

NAME & SIGNATURE:_____ _____

APPROVED BY THE RPO DATE

NAME & SIGNATURE:_____ _____